Author/s:
Gao, C;Wong, WWH;Qin, Z;Lo, SC;Namdas, EB;Dong, H;Hu, W

Title:
Application of Triplet–Triplet Annihilation Upconversion in Organic Optoelectronic Devices: Advances and Perspectives

Date:
2021-11-01

Citation:
Gao, C., Wong, W. W. H., Qin, Z., Lo, S. C., Namdas, E. B., Dong, H. & Hu, W. (2021). Application of Triplet–Triplet Annihilation Upconversion in Organic Optoelectronic Devices: Advances and Perspectives. Advanced Materials, 33 (45), pp.e2100704-. https://doi.org/10.1002/adma.202100704.

Persistent Link:
https://hdl.handle.net/11343/299048

Application of triplet-triplet annihilation upconversion in organic optoelectronic devices: advances and perspectives

Can Gao, Wallace W. H. Wong, Zhengsheng Qin, Shih-Chun Lo, Ebinazar B. Namdas, Huanli Dong, Wenping Hu*

Dr. C. Gao, Z. Qin, Prof. H. Dong

Beijing National Laboratory for Molecular Sciences, Key Laboratory of Organic Solids, Institute of Chemistry, Chinese Academy of Sciences, Beijing 100190, China

E-mail: dhl522@iccas.ac.cn

Z. Qin

University of Chinese Academy of Sciences, Beijing 100049, China

Dr. W. W. H. Wong

ARC Centre of Excellence in Exciton Science, School of Chemistry, Bio21 Institute, The University of Melbourne, Melbourne, Victoria 3010, Australia

Prof. S.-C. Lo

Centre for Organic Photonics & Electronics, School of Chemistry and Molecular Biosciences, The University of Queensland, Brisbane, QLD 4072, Australia

Prof. E. B. Namdas

This is the author manuscript accepted for publication and has undergone full peer review but has not been through the copyediting, typesetting, pagination and proofreading process, which may lead to differences between this version and the Version of Record. Please cite this article as doi: 10.1002/adma.202100704.

Centre for Organic Photonics & Electronics, School of Mathematics and Physics, The University of Queensland, Brisbane, QLD 4072, Australia

Prof. W. Hu

Tianjin Key Laboratory of Molecular Optoelectronic Science, Department of Chemistry, School of Science, Tianjin University, Tianjin 300072, China

Keywords: triplet-triplet annihilation, upconversion, organic optoelectronic devices, high mobility, efficient triplet exciton utilization

Abstract: Organic semiconductor materials have been widely used in various optoelectronic devices due to their rich optical and/or electrical properties, which are highly related to their excited states. Therefore, how to manage and utilize the excited states in organic semiconductors is essential for the realization of high-performance optoelectronic devices. Triplet-triplet annihilation (TTA) upconversion is a unique process of converting two non-emissive triplet excitons to one singlet exciton with higher energy. Efficient optical-to-electrical devices can be realized by harvesting sub-bandgap photons through TTA-based upconversion. In electrical-to-optical devices, triplets generated after the combination of charges and holes also can be efficiently utilized via TTA, which resulted in a high internal conversion efficiency of 62.5%. Currently, many interesting explorations and significant advances have been demonstrated in these fields. In this review, a comprehensive summary of these intriguing advances on developing efficient TTA upconversion materials and their application in optoelectronic devices is systematically given along with some discussions. Finally, the key challenges and perspectives of TTA upconversion systems for further improvement for

optoelectronic devices and other related research directions are provided. This review hopes to provide valuable guidelines for future related research and advancement in organic optoelectronics.

Keywords: triplet-triplet annihilation, upconversion, organic optoelectronic devices, high mobility, efficient triplet exciton utilization

1. Introduction

The discovery of high electrical conductivity of polyacetylene by Alan Heeger, Hideki Shirakawa, and Alan MacDiarmid in 1976 opened up the new research field of organic optoelectronics.[1] Organic optoelectronic materials, based on organic small molecules and conjugated polymers, exhibit unique properties compared with their inorganic counterparts, such as rich optical and electronic properties, low-cost, high flexibility, light-weight, solution processability, *etc*., have been widely used to fabricate organic optoelectronic devices.[2-11] Thanks to the rapid development of new organic semiconductor materials in the past decades, remarkable advancements have been achieved in optoelectronic devices. For example, the maximum power conversion efficiency (PCE) of organic photovoltaic devices has surpassed 18%.[12-15] The organic light-emitting diodes (OLEDs) have been successfully commercialized as displays for high-end mobile phones and TVs. The charge-carrier mobility of organic semiconductors in organic field-effect transistors (OFETs) has increased from the initial 10^{-5} cm^2 V^{-1} s^{-1} to current values of over 40 cm^2 V^{-1} s^{-1}.[16-18] Recently, organic light-emitting

transistors (OLETs), with potential to be the smallest integrated optoelectronic device, have attracted much attention due to their dual ability in switching as OFET and light emission as OLED in a single device.[19-21] OLET devices show great potential to simplify the existing optoelectronic device structures and boost the development of photonic communications and electronically pumped organic lasers.[22-25] These substantial achievements for all the optoelectronic devices are attributed to the good understanding of the intrinsic electronic and optical properties involving rich excited states in organic semiconductors.

For organic semiconductor molecules, the fluorescent singlet excited-state has been investigated intensively since the first report of electroluminescence in organic materials.[26, 27] In contrast, the emission from a triplet excited-state in purely organic semiconductors, *i.e.* phosphorescence, is usually very weak due to the spin forbidden transition to the ground state.[28, 29] The triplet excited-states remained more elusive until the improvements in detection technology, especially the development of organometallic complexes made the triplet excited-states more easily accessible for spectroscopic investigation and technological exploitation.[30, 31] Since then, more and more attention has been paid to the investigation of triplet excitons in various related areas.[32-36] Properly adjusting and utilizing the triplet excitons in organic semiconductors have significant effects on promoting the performance of optoelectronic devices and broadening their applications in more advanced areas. For instance, exciton diffusion length is one of the common factors to impact the PCE of bulk-heterojunction photovoltaics. Triplet excitons are attractive for organic photovoltaics to enhance the exciton dissociation for free charges generation due to their long-lived lifetime and long diffusion length.[37-39] For single-junction photovoltaics, the maximum theoretical conversion efficiency is limited to 33.7% [also known as Shockley-Queisser (SQ) limit] under the standard

AM1.5G spectrum. This is mainly due to two main losses: the photons with energy exceeding the threshold are lost through thermalization, while the sub-bandgap photons cannot be absorbed at all.[40-42] Photon upconversion and singlet fission (SF) which involving triplet excitons are considered promising approaches to break the SQ limit.[43-47]

In contrast to photovoltaic devices, OLEDs and OLETs convert electricity to light. In OLEDs and OLETs, 25% singlets and 75% triplet excitons are generated *via* electron-hole recombination through charge injections from the electrode contacts. Since the out-coupling efficiency is normally below 20%, the maximum external quantum efficiency (EQE) of fluorescent materials-based OLEDs and OLETs is limited to 5%.[48] Apparently, the fraction of triplet excitons seriously limited the efficiency of these electrical-to-optical devices. Intensive efforts have been made to improve device EQEs by harvesting triplet excitons, such as developing materials with properties of phosphorescence, triplet-triplet annihilation (TTA), thermally activated delayed fluorescence (TADF), hybridized-local and charge transfer states (HTLC), hot excitons, and radicals.[31, 49-61] As a result, harvesting triplet excitons plays an essential way to improve the performance of OLEDs and OLETs.[62-65]

Amongst these approaches, triplet-triplet annihilation (TTA) upconversion, also known as triplet fusion (TF) upconversion, is a unique process of converting two triplet excited-states which leads to the formation of one singlet excited-state. This allows for photon upconversion, where light of long wavelength is converted to photons with higher energy. Since the first report by Parker and Hatchard in 1962[66], TTA upconversion has attracted significant attention due to its unique advantages, such as high upconversion quantum yield, low excitation intensity requirement (a few mW cm^{-2} is sufficient for upconversion), and readily tunable excitation/emission wavelength.[67-70] Thus, TTA upconversion has numerous potential applications in bio-imaging, sensing, photocatalysis

and optoelectronic devices.[71-77] In addition, photon upconversion has long been considered as a potential mechanism for solar cells to harvest sub-bandgap photons, which may exceed the imposed SQ limit.[46, 78-81] Incorporating an upconverting layer into a single junction photovoltaic device will increase the maximum theoretical efficiency under one sun illumination from ~33% to ~45%, and allow the use of wider bandgap materials.[40, 46]

For OLEDs and OLETs based on TTA materials, the internal conversion efficiency of up to 62.5% may be possible.[82, 83] Though the maximum internal conversion efficiency is not as high as other materials (such as phosphorescent and TADF molecules), TTA has attracted much attention owing to its inherent merits, such as efficient blue emission, small efficiency roll-off, low operation voltage, and low cost.[84-91] Efficiency roll-off in electroluminescence devices means the device efficiency decreases as the brightness increases, which may be caused by singlet-triplet annihilation, singlet-polaron annihilation, and loss of charge carrier balance, *etc*.[92] Moreover, the unique structure of most TTA materials with relatively rigid conjugation enables their possibility for integrating high carrier mobility and efficient triplet utilization in one molecule, which are attractive for the fabrication of high performance single component OLETs.

In the past decades, many great efforts have been made to improve the efficiency of TTA upconversion and their corresponding optoelectronic devices. Some excellent reviews have been given in literatures with special focus on active materials, working mechanism and device architectures, *etc*.[40, 80, 81, 93-100] Until now, there have been no comprehensive reviews on current progress on applications of TTA upconversion in optoelectronic devices. In this review, we will give a timely comprehensive summary and brief discussions of these fantastic advancements on the

development of efficient TTA upconversion material systems and their applications in organic optoelectronic devices. An overview of the review content is summarized in **Figure 1**, which includes two working processes of optical-to-electrical conversion and electrical-to-optical conversion correlated with three typical optoelectronic devices, including photovoltaics, OLEDs and OLETs. In the first section, we will give a brief description of the basic working mechanism and statistics of TTA upconversion process, which is followed by conclusion of advanced solution and solid-state optical TTA upconversion systems. The applications of TTA upconversion in photovoltaic devices, OLEDs and OLETs will be extensively discussed. This includes selections of active materials for TTA upconversion, device architectures and performances. Finally, the challenges and perspective of TTA upconversion systems for further improvement of optoelectronic devices and other related research directions are provided.

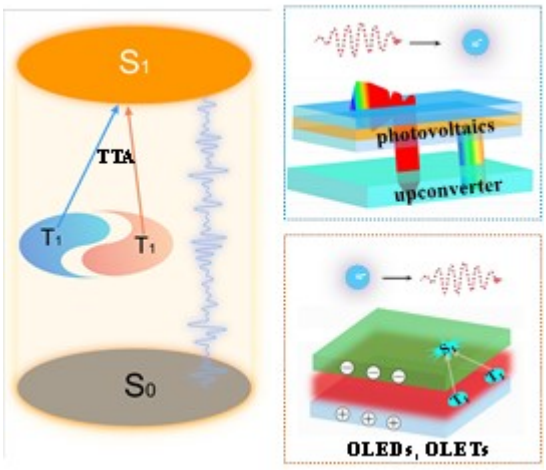

Figure 1. Illustration of TTA process and applications of TTA in optoelectronic devices, including photovoltaics, OLEDs and OLETs.

2. TTA upconversion mechanism and figures of merit

Typically, two components are involved in optical pumped TTA upconversion systems: a sensitizer (S) with narrow optical gap and a TTA annihilator/emitter (A/E). A triplet sensitizer molecule can be excited to its singlet excited-state by absorbing low energy photons. Following, this singlet excited-state is quickly converted to its triplet excited-state (^{3}S*) through intersystem crossing (ISC) as illustrated in **Figure 2a**. The energy in triplet excited-state sensitizer is transferred to an annihilator molecule through triplet energy transfer (TET) to form triplet species (^{3}A*). With a sufficiently high triplet population on the annihilator molecules, two or more triplets (^{3}A*) can interact to produce one annihilator in its ground state (^{1}A) and one in the singlet excited-state (^{1}A*). Finally, the singlet excited-state (^{1}A*) of the annihilator decays radiatively back to its ground state by producing a photon with higher energy than those initially absorbed by the sensitizer molecule (**Figure 2a**). For electrical pumped TTA upconversion, 25% singlets and 75% triplets are generated after the combination of electrons and holes based on the spin statistics in the device. However, triplet excited state to singlet ground state transitions are spin forbidden and consequently cannot emit light in fluorescent materials, which seriously limits the electrical-to-optical conversion efficiency. These dark triplets can be upconverted to a bright singlet through TTA, leading to delayed electroluminescence (EL) as shown in **Figure 2b**.

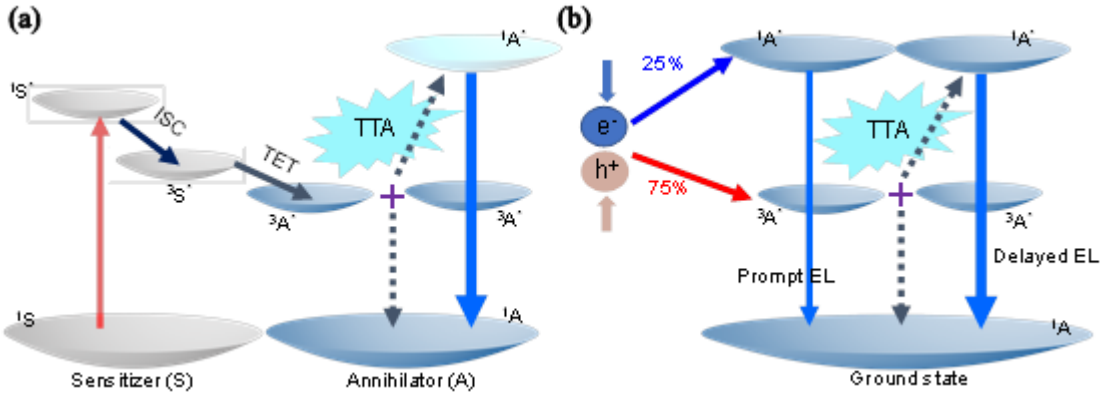

Figure 2. Working mechanism of (a) optical-pumped TTA and (b) electrical-pumped TTA processes.

TTA is the process of interactions between two annihilators in their first triplet excited-state which forms encounter complexes of singlet, triplet and quintet with spin multiplicities of 1/9, 3/9 and 5/9, respectively (as shown in Equations 1, 2 and 3).

$$^3A^* + {}^3A^* \leftrightarrow {}^1(AA)^* \rightarrow {}^1A^* + {}^1A \quad (1)$$

$$^3A^* + {}^3A^* \leftrightarrow {}^3(AA)^* \rightarrow {}^3A^* + {}^1A \quad (2)$$

$$^3A^* + {}^3A^* \leftrightarrow {}^5(AA)^* \rightarrow {}^5A^* + {}^1A \quad (3)$$

where $^3A^*$ is the triplet excited-state, $^1(AA)^*$ is the singlet encounter complex, $^3(AA)^*$ is the triplet encounter complex, $^5(AA)^*$ is the quintet encounter complex and ^1A is the ground state of annihilator. In this case, only the singlet encounter complexes can undergo internal conversion to the singlet excited state ($^1A^*$) which emits light. Therefore, the maximum TTA efficiency is expected to be 11.1% (*i.e.*, 1/9) according to the spin statistics.[101, 102] However, this spin-statistic limit has been disproven through various ways.[103-105] Firstly, the quintet encounter complex acquires much higher energy than the singlet excited-state energy and two times of the triplet excited-state energy.

Therefore, the route through Equation 3 is inaccessible and the quintet encounter complex dissociates back to the initial triplet excited-states. Usually, the triplet encounter complex can produce a higher triplet excited-state (*e.g.*, the second triplet excited-state, $^3A^{2*}$), which can undergo fast relaxation to $^3A^*$. This implies that for the two $^3A^*$ consumed through Equation 2, one returned will be available again to undergo further TTA. In this case, the maximum TTA efficiency will exceed 40%.[106-109]

TTA shows non-linear optical property as bimolecular interactions are involved in this process. The annihilators in triplet excited-states ($^3A^*$) decay through two competing pathways, as shown in Equation 4:[96, 110-112]

$$\frac{d[\,^3A^*]}{dt} = -k_T[\,^3A^*]_t - k_{TT}[\,^3A^*]_t^2 \quad (4)$$

where k_T is the sum of all first order and pseudo-first order decay constant, k_{TT} is the second order rate constant of TTA.

In the weak annihilation regime, where the excitation intensity is low, k_T is much larger than $k_{TT}[^3A^*]$, the dynamics of annihilator triplet excited-states is dominated by spontaneous nonradiative decay where TTA is inefficient. Therefore, the upconverted emission intensity *I* is proportional to $[^3A^*]^2$ as shown in Equation 5, and *I* is quadratically dependent on the excitation intensity.

$$I = \frac{\Phi_{PL}k_{TT}[\,^3A^*]_0^2}{2k_T} \quad (5)$$

Under high excitation intensity conditions, while the annihilation is strong, k_T is much smaller than $k_{TT}[^3A^*]$. Therefore, *I* is proportional to $[^3A^*]_0$ as shown in Equation 6 and shows a linear relationship with the excitation intensity.

$$I = \Phi_{PL}[\,^3A^*]_0 \quad (6)$$

As shown in **Figure 3a,** the slope changes from 2 to 1 in a log-log plot in both optically-pumped and electrically-pumped TTA systems.[111, 113] The crossing point of the two different slope lines corresponds to the value of excitation threshold (I_{th}), which is an important figure-of-merit to judge the performance of TTA upconversion system.[69, 108, 114, 115] Above the I_{th} value, the upconversion quantum yield (Φ_{UC}) and EQE reaches and maintains their maximum value (**Figure 3b**).

The TTA-based photon upconversion quantum yield (Φ_{UC}) represents the number of photons with high-energy emitted by annihilators compared to the number of photons with low-energy absorbed by sensitizers, which is one of the most important parameters to evaluate the efficiency of TTA-based photon upconversion systems. Φ_{UC} is related the efficiency of ISC, TET, TTA and fluorescence (FL) process, as shown in Equation 7:

$$\Phi_{UC} = \Phi_{ISC}\Phi_{TET}\Phi_{TTA}\Phi_{FL} \quad (7)$$

where Φ_{ISC}, Φ_{TET}, Φ_{TTA}, Φ_{FL} are the quantum yield of ISC of the sensitizer, the quantum efficiency of TET from the triplet excited-state sensitizer to the annihilator, the quantum efficiency of TTA between two annihilators in their triplet excited-states, and the fluorescence quantum yield of the annihilator, respectively.

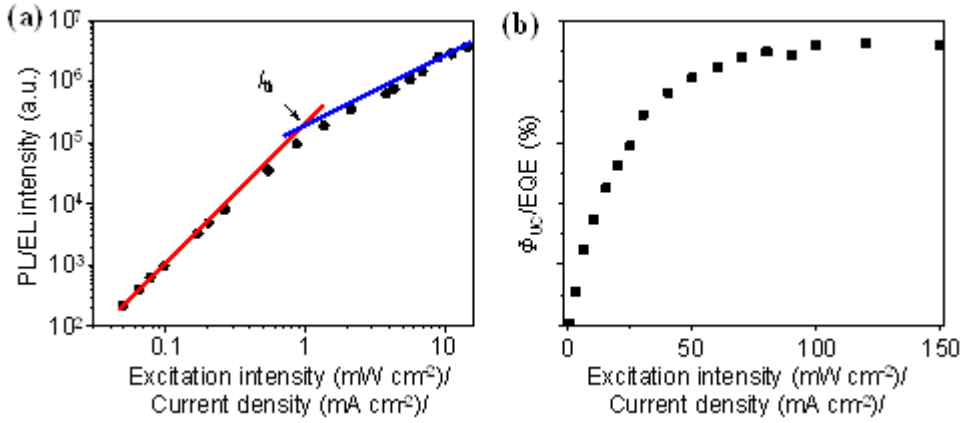

Figure 3. (a) Photoluminescence (PL)/electroluminescence (EL) emission intensity and (b) Φ_{UC}/EQE as a function of excitation intensity/current intensity.

3. Photovoltaics assisted by TTA upconversion systems

Solar energy is receiving increasing attentions as an abundant, clean and renewable energy form. Solar cells, an electrical device that directly converts sunlight to electricity, have been developed rapidly in recent decades. The first generation solar cells which are made of crystalline silicon have been successfully commercialized and make up a major part of the photovoltaic market.[116] However, these solar cells are manufactured by pure silicon, the cost of generating crystalline silicon is high compared to their power output.[116] To reduce the cost of the first generation solar cells, the second generation solar cells based on thin film technologies have been developed, which encompass amorphous silicon (a-Si), copper indium gallium di-selenide, cadmium telluride solar cells.[117] However, all of these solar cells are of single threshold type which suffer from SQ limit due to the transmission and thermalization energy losses.[40] For many second generation solar cells, their ability to harvest sunlight above 800 nm is poor.[118] Therefore, their energy conversion

efficiency can be further improved if the sub-bandgap photons can be harvested efficiently. Thus, the third generation solar cells have been developed to further improve the energy conversion efficiency and reduce the cost through several approaches, such as developing new active materials, innovating new device architectures and converting incident spectrum, *etc*.[15, 119] Amongst these approaches, photon upconversion based on TTA has attracted intense attention in recent years which has been readily utilized into solar cells for harvesting sub-bandgap photons. In this section, we will summarize the state-of-the-art of TTA upconversion systems and their applications in solar energy conversion.

As shown in **Figure 4a**, sub-bandgap photons from sunlight can be absorbed and upconverted to excitons with higher energy through TTA in solar cells. Incorporating TTA upconversion into photovoltaic devices is desirable to boost the solar energy conversion efficiency and therefore decrease the cost. Up to now, efficient TTA upconversion has been realized in dilute solution due to the fast molecular diffusion rate, which is favorable for efficient TET and TTA. However, considering practical applications, more and more attention has been paid into the development of solid-state TTA upconversion systems under low excitation intensity. According to the structures of incorporated solar cells, TTA upconverter can be integrated to the solar cells optically and electrically (**Figure 4b** and **4c**). In optically integrated solar cell (**Figure 4b**), the TTA upconversion layer is working independently in the rear part of the solar cell with a reflector. In the electrically integrated solar cell (**Figure 4c**), the energy from upconverted singlet is directly injected into the electrode before light emission. Continuous efforts on developing efficient TTA upconversion systems and TTA-integrated solar cell devices have been made. The basis of improving upconversion incorporated solar cells is dependent on improving upconversion chromophores, therefore, this section will firstly

summarize the main requirements for designing upconversion chromophores. Then, the state-of-the-art of TTA upconversion systems in solution and solid-state, as well as their applications in solar energy harvesting will be summarized and discussed.

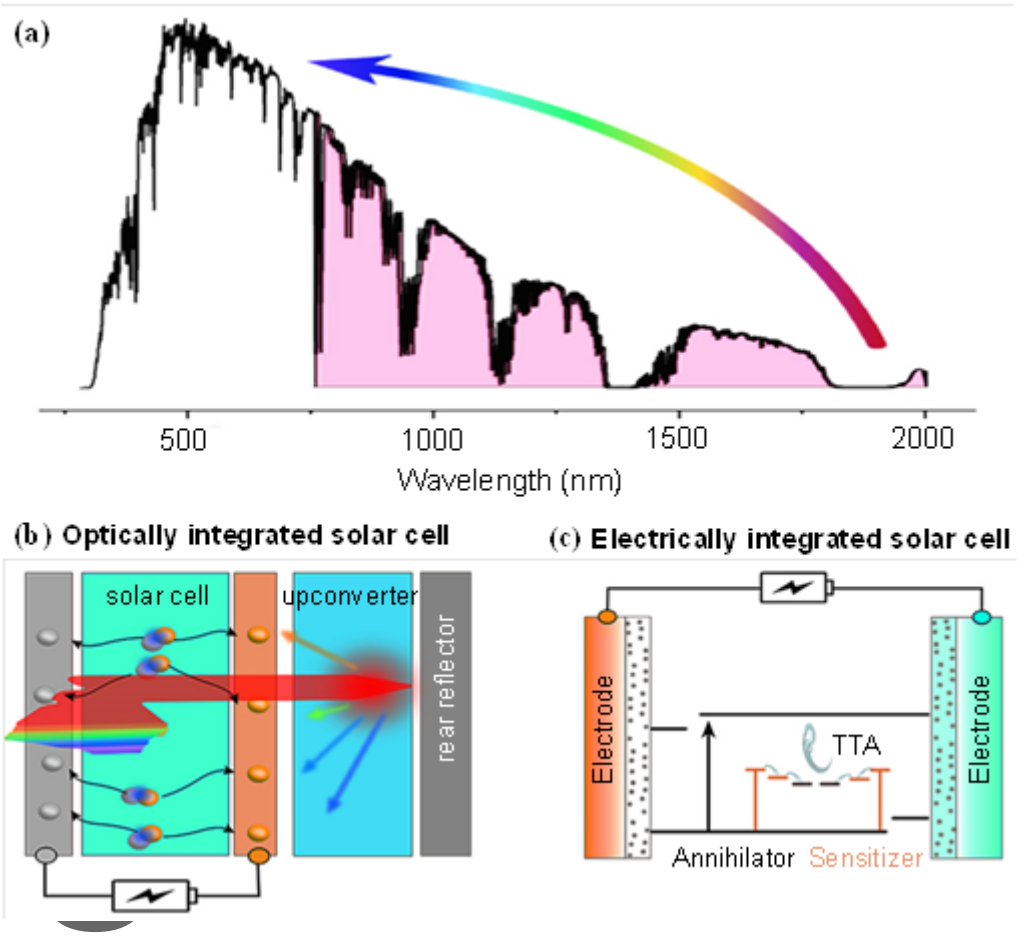

Figure 4. (a) 1.5 AM sunlight spectrum with highlighted parts for upconversion. Schematic illustrations of (b) an optically integrated solar cell and (c) an electrically integrated solar cell.

3.1 Selection of active materials for TTA upconversion

Triplet excitons cannot be directly generated by optical excitation without effective ISC through efficient spin-orbital coupling of heavy metal effect because it is spin-forbidden process. Hence, to give efficient TTA upconversion through optical pumps, sensitizers are required to absorb low energy photons and create triplet excitons. Accordingly, the sensitizers should have 1) a strong absorption in the desired spectral region; 2) a high ISC efficiency; 3) a long triplet lifetime and finally 4) a small singlet-triplet energy gap to minimize the energy loss during the ISC process. According to these above requirements, many materials including heavy-metal complexes, organic dyes (including TADF materials), quantum dots (QDs) and perovskite have been successfully developed as triplet sensitizers for efficient TTA upconversion.[95, 120-129] Charge transfer states between electron donor and acceptor moieties can also act as sensitizers.[130, 131] For an efficient TTA upconversion system, the annihilators should meet below requirements: 1) a singlet energy level at just below two times of the first excited triplet state energy level; 2) a long triplet lifetime; 3) the second triplet excited-state should not be energetically accessible from the TTA event to ensure high TTA yields. Based on these requirements, polycyclic aromatic hydrocarbon acenes (including anthracene, pyrene, perylene, tetracene, rubrene and their derivatives) have been widely used as the annihilators for TTA upconversion.[98, 132-138] Some commonly used sensitizers and annihilators discussed in this article are summarized in **Figure 5**.

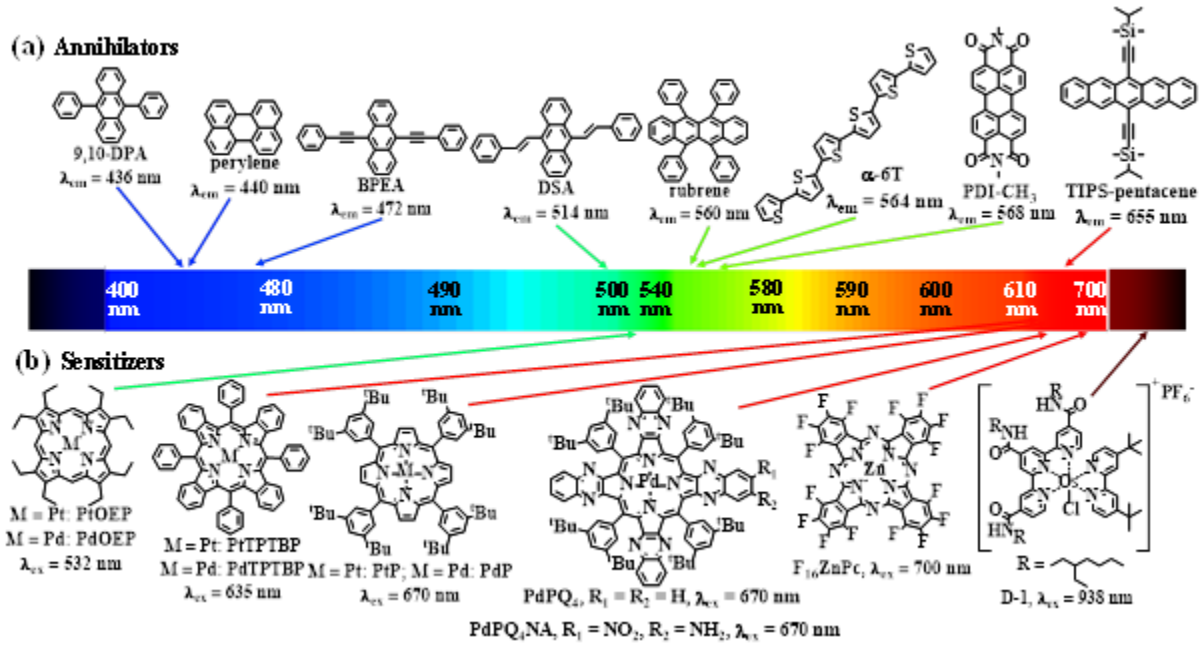

Figure 5. Chemical structures of commonly used (a) annihilators and (b) sensitizers from literatures.

3.2 Incorporating solution-based TTA upconversion systems into photovoltaics

The simplest way to realize optically-pumped TTA upconversion is to dissolve the sensitizer and annihilator in a suitable organic solvent[139], such as toluene,[132] benzene,[101] chloroform,[140, 141] acetonitrile,[121, 142] dimethyl formamide,[143] *etc*. Up to now, most of the efficient TTA upconversion systems have been demonstrated in solution since both the TET and TTA processes are diffusion control. The solution-based environment can significantly facilitate the chromophore diffusion and provide a good testing platform for new TTA upconversion systems.[69, 144] Towards to the application, the first TTA upconversion incorporated solar cell devcie was demonstrated by Schmidt *et al.* in 2012. After continuous efforts in recent years, the performance of solution-based TTA upconversion incorporated solar cells has been largely improved.

3.2.1 Development of solution-based TTA upconversion systems

Even though the highest solution TTA upconversion efficiency of over 38% (out of a 50% maximum) has been reported for green-to-blue conversion, the upconversion efficiency for NIR-to-red light conversion is much lower, which is more required for some applications[109]. Hence, it is of significance to effectively harvest red/NIR through TTA upconversion for solar cells applications. However, it is still challenging as most sensitizers used in TTA upconversion showed poor absorption efficiency in the red/NIR region. To date, porphyrin-like centre with extended conjugated frameworks, quantum dots, TADF and perovskite sensitizers have been reported to exhibit upconversion from visible to the red/NIR region.[122, 124, 127, 145-148] The upconversion efficiencies of these systems are still needed to be improved to meet the application in such as solar cells.

3.2.2 Solution-based TTA upconversion systems integrated photovoltaics

Incorporating TTA upconversion into photovoltaics has attracted increasing attentions in recent years which are mainly attributed to its ability in harvesting the sub-bandgap photons. In this section, solution-based TTA upconversion integrated solar cell systems will be summarized and discussed in detail.

Integration of TTA upconversion into solar cell devices optically is a relatively simple approach to implement with several notable advantages. For instance, they can build on already available and high efficiency solar cells, which could greatly simplify the manufacture steps. In addition, the performance and components of the upconversion layer and the solar cell can be optimized and tuned independently. In this case, all the already available highly efficient TTA upconversion chromophores can be choose and utilized in these devices.

Schmidt group has demonstrated many TTA upconversion integrated solar cell systems, including hydrogenated amorphous silicon (a-Si:H) soalr cell, organic photovoltaics and dye-sensitized solar cell (DSSC) device. A figure of merit (FoM, $\xi = \Delta J_{SC}\ C^{-2}$) was introduced by them to compare the photocurrent enhancement between these systems, where ΔJ_{SC} is total short circuit current density increase and *C* is the effective solar concentration. In the first TTA upconversion integrated a-Si:H, red-absorbing sensitizers ($PdPQ_4$ or $PdPQ_4NA$, **Figure 5b**) and annihilator (rubrene, **Figure 5a**) were sealed in a 1 cm pathlength air-free cuvette and mounted on the backside of the solar cell device.[149] The FoM of solar cell with upconverter was calculated of 2.8×10^{-5} mA cm^{-2} sun^{-2} and 1.3×10^{-4} mA cm^{-2} sun^{-2} for the PQ_4Pd and PQ_4PdNA systems, respectively. Further improvement was obtained by using an organic solar cell with a higher external quantum efficiency and high transmission of red light at 670 nm.[78] Quantum efficiency of this organic solar cell device showed significant improvement with the upconversion layer compared to that without upconversion. A FoM of 1.60×10^{-4} mA cm^{-2} sun^{-2} was obtained in P3HT:ICBA organic solar cell. Meanwhile, a comparison a-Si:H solar cell was prepared by increasing the light transmission in the 670 nm region, a FoM of 7.63×10^{-4} mA cm^{-2} sun^{-2} was achieved, which is about 27 times higher compared to that of above-mentioned PQ_4Pd system assisted a-Si:H solar cell.

Since the upconversion emission is isotropic, more than half of the upconverted emission is lost as it is emitted away from the solar cell.[118] To overcome this issue, Schmidt *et al.* placed a Lambertain reflector to further improve the harvesting of the upconverted light by the solar cell layer.[118] As a result, a FoM of 1.7×10^{-4} mA cm^{-2} sun^{-2} and 4.9×10^{-4} mA cm^{-2} sun^{-2} were obtained for uponconverters with and without silver-coated glass spheres, respectively. Consequently, a fully integrated upconversion DSSC device was reported.[150] The solution-based upconversion system

consisting of $PdPQ_4NA$ and rubrene was contained within the encapsulated chamber, and a Al_2O_3 reflector was placed in the rear part of the device (**Figure 6a**). The upconverted emission was captured by the D149 dye (**Figure 6b**) for high efficiency DSSC. This device displayed a FoM of 2.5 × 10^{-4} mA cm^{-2} sun^{-2} under sub-bandgap illumination at low excitation fluence. In 2016, the FoM was further increased to 4.5 × 10^{-3} mA cm^{-2} sun^{-2} for DSSC by employing a dual-annihilator TTA upconversion system.[71] Rubrene and 9,10-bis(phenylethynyl)anthracene (BPEA, **Figure 5a**) were selected as the annihilators with PQ_4PdNA as the sensitizer. In this dual-annihilator upconversion system, parasitic absorption was successfully avoided as the emission from rubrene is within the absorption window of the sensitizer and the emission spectrum matches well with the integrated solar cell spectral responses.

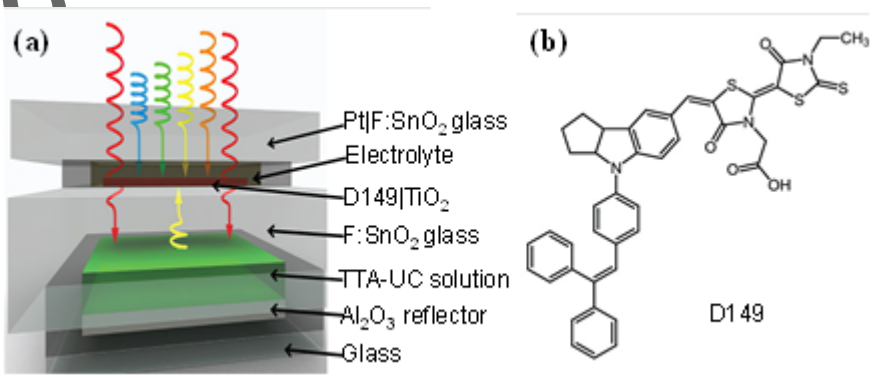

Figure 6. (a) Device structure of the upconversion-integrated DSSC. (b) Molecular structure of D149. Reproduced with permission.[150] Copyright 2013, American Chemical Society.

Up to now, the photocurrent efficiency of solution-based TTA upconversion integrated solar cell has been enhanced for several times. However, this strategy also has many problems, such as the

relatively low sensitizer concentration, which resulted in limited absorption of sub-bandgap photons. In addition, energy losses, caused by sensitizer-sensitizer annihilation and parasitic energy transfer, are dentrimental to the upconversion efficiency. Therefore, more attentions are needed to be paid on these issuses to further harness TTA upconversion in solar cells.

3.3 Incorporating solid-state TTA upconversion systems into photovoltaics

Although efficient TTA upconversion has been achieved in solution and successfully integrated into solar cell devices, the use of volatile organic solvents is not practical for device engineering. For incorporation of TTA upconversion with solar cell devices, it is still desired to develop efficient solid-state upconverters under low excitation intensity.

3.3.1 Development of solid-state TTA upconversion systems

As the triplet excited-states are sensitive to oxygen molecules, various matrix were utilized to protect the sensitizer and annihilator from oxygen quenching. Hence, an approach of encapsulating organic liquids containing sensitizers and annihilators have been developed.[72, 151-155] However, seals are easily dissolved and broken, which dramatically limited the practical applications. To meet the requirements of device engineering, rubbery polymers and rigid polymers have been widely used as the host matrix to serve as a mechanical support for the upconversion pairs and also block oxygen.[156-170] In addition, solid-state TTA upconversion systems were also reported in metal-organic frameworks (MOFs).[81, 96, 99] Solid-state TTA upconversion systems have been well summarized in many reviews from different aspects.[79, 96, 171]

In 2007, Weder, Castellano and co-workers represented the first example of green-to-blue solid-state TTA upconversion system in a rubbery polymer film by using palladium octaethylporphyrin

(PdOEP, **Figure 5b**) and 9,10-diphenyl anthracene (9,10-DPA, **Figure 5a**) as sensitizer and annihilator, respectively.[156] Lately, various solid-state upconversion systems have been reported by blending upconversion pairs in different polymer matrix, such as polyurethane[157], polyethylene glycol[158], poly(methylmethacrylate)[159], and cellulose acetate[172]. In 2012, Monguzzi *et al.* obtained TTA upconversion efficiency of 3.0% and 3.7% in platinum octaethylporphyrin (PtOEP, **Figure 5b**)/ 9,10-DPA-doped polystyrene nanoparticle aqueous suspension and drop-cast films, respectively.[165] The TTA upconversion efficiency was further increased to 11% with a low excitation threshold of 20 mW cm^{-2} by Castellano *et al.*[161] The benchmark green-to-blue TTA upconversion pair (PdOEP/9,10-DPA) was blended into transparent and flexible rubbery solids fabricated by using commercially available polyurethane precursors (Clear Flex 50, CLRFLX). High 9,10-DPA and PdOEP concentrations were used to realize efficient TET and TTA as chromophore diffusion was restricted in the polyurethane matrix. The formation of micrometer particles containing 9,10-DPA and PtOEP in polyurethane was confirmed by Wong, Smith and co-workers.[136, 137] This procedure was lately extended to a dual-sensitizer system for broadband light absorption. The dual-sensitizer of PdOEP and PdTPTBP enabled the absorption of more photons both in red and green, which enhanced the overall upconversion efficiency.[173] In 2016, groups of Bulović, Bawendi and Baldo reported a solid-state NIR-to-vis TTA upconversion.[174] A mixture of energy collector (rubrene) and annihilator (dibenzotetraphenylperiflanthene, DBP) was vacuum deposited on a PbS nanocrystal. PbS nanocrystal absorbed NIR light (1010 nm) and transferred excited-state energy to rubrene, where upconverted emission peak at 612 nm from DBP was observed.

Recently, Kimizuka and Yanai groups have reported various solid-state TTA upconversion systems.[99, 100, 175-184] A concept of triplet energy migration was proposed to solve the restricted

molecular diffusion issue in solid-state environments.[100, 183] In 2015, they developed the self-assembled nanofibers as oxygen barrier matrix.[178] The gel nanofibers accumulating various sensitizer-annihilator upconversion pairs were prepared, exhibiting air-stable and strong TTA upconverted emissions from visible to UV range. To realize NIR-to-vis upconversion, an osmium complex, Os(atpy)(tbbpy)Cl^+ (atpy = tris(2-ethylhexyl)-[2,2':6',2''-terpyridine]4,4',4''-tricarboxamide; tbbpy = 4,4'-di-tert-butyl-2,2'-bipyri-dine) (D-1, **Figure 5b**), with branched alkyl chains was designed as a sensitizer to be miscible with the nonpolar annihilator rubrene.[185] The strong spin-orbit coupling of the Os complex enabled the direct singlet-to-triplet absorption and reduce energy loss during triplet sensitization. Amorphous upconversion nanoparticles consisting of D-1 and rubrene was prepared through reprecipitation method. The obtained nanoparticles were dispersed in poly(vinyl alcohol) (PVA) to protect the triplets from oxygen quenching. Under the excitation of NIR light (980 nm), bright yellow light (580 nm) was observed from the solid film even under ambient conditions. A maximum upconversion efficiency of ~1.55% (out of a 50% maximum) was achieved from the D-1-doped rubrene nanoparticle in PVA film under the photoexcitation in air.

Crystalline solids including sensitizer and annihilator have also been developed and studied for efficient solid-state TTA upconversion.[177, 186] In 2017, red-to-green upconversion nanocrystals were prepared by Li *et al.* using 9,10-distyrylanthracene (DSA, **Figure 5a**) and PdTPTBP (**Figure 5b**) as the annihilator and sensitizer, respectively.[187] An Φ_{UC} of 0.29% was obtained under an excitation intensity of 120 mW cm^{-2} at 640 nm. Lately, upconversion crystals containing PtOEP, DPA and its derivatives were prepared by Gao *et al.* with a ratio of 1:800.[137] Uniform upconversion crystals were formed by reprecipitation methods. The bright blue upconverted emission intensity from PtOEP-DPA and PtOEP-bDPA crystals increased as increasing the excitation power intensity at 532 nm. PtOEP-

bDPA crystals showed more efficient TET and TTA upconversion efficiencies than that of PtOEP-DPA crystals, which were attributed to the better distribution of PtOEP in bulky- DPA crystals. As a result, almost 50 times higher upconversion efficiency compared to that of PtOEP-DPA crystals was obtained. Moreover, the crystalline TTA upconversion systems show improved air-stability as the tight molecular packing can block oxygen well. The excellent performance of crystalline TTA upconversion systems exhibit the potential to harvest sunlight in solar cell devices.

3.3.2 Solid-state TTA upconversion integrated photovoltaics

For long-term practical applications, solid-state TTA upconversion systems are more desirable to be integrated into photovoltaic devices for harvesting sub-bandgap light. Solid-state TTA upconversion systems have been integrated into optically and electrically solar cells, including DSSCs and organic photovoltaics.

In this section, we will firstly discuss the optically integrated solar cell systems. In 2016, the first solid-state TTA upconversion polymeric film integrated DSSC device was reported by Kim, Schmuttenmaer and their co-workers.[188] TTA upconversion films were fabricated using polyurethane as the matrix to block oxygen with PdTPTBP (**Figure 5b**) as the sensitizer and perylene (**Figure 5a**) as the annihilator. This upconversion system show good absorption at 635 nm and red-to-blue upconversion with good air stability. When coupled this TTA upconversion film and a reflector with a DSSC device which has a 5 μm TiO_2 layer, a maximum photocurrent enhancement of 37.3% was realized under one-sun illumination compared to the initial photocurrent of 9.8 mA cm^{-2}. The first TTA-based organic photovoltaics was fabricated by Rand *et al.* in 2017.[189] A material system consisting of PtTPTBP as the triplet sensitizer, and α-sexithiophene (α-6T, **Figure 5a**) and

diindenoperylene (DIP) as the annihilator and energy acceptor, respectively, was strategically selected to meet the energetic requirements of the organic photovoltaic. Triplets populated in α-6T after TET from PtTPTBP was evidenced by transient absorption spectroscopy, while TTA upconverted emission showing quadratic dependence on excitation power was confirmed by delayed fluorescence spectroscopy. The photocurrent enhancement of this device was only 0.013 mA cm^{-2}. The low photocurrent enhancement was attributed to low TTA efficiency and back energy transfer from annihilator to sensitizer. For further improve the device efficiency, the authors proposed to incorporate a sensitizer host with slightly higher triplet energy for preventing back energy transfer.

Apart from using the back reflector to redirect the upconverted light back toward to solar cell device, another approach is to use waveguide. Luminescent solar concentrator (LSC) is a light-harvesting device containing fluorophores that absorb light over the large surface area of a planar waveguide.[190-193] In 2018, Reichmanis, Moon and their co-workers fabricated a dual-band LSC device to harvest both ultraviolet and red visible light through downconversion and upconversion processes, respectively (**Figure 7a** and **7b**). The upconversion LSC luminesces high energy green light from BPEA (annihilator, **Figure 5a**) by absorbing low energy red light through PdTPTBP (sensitizer), as well as downshift LSC that luminescence green light by absorbing ultraviolet light.[194] The luminescent light concentrated from the two LSCs is absorbed by a DSSC having a high extinction coefficient at this wavelength. A PCE of 6.1% was obtained from the optimized dual band LSC-SC, which was 13% higher than that of the single band LSC-SC (5.4%). The PCE was further increased to 7.8% by changing the downconversion material of BPEA to anthracene (**Figure 7c**).[195] The average visible transmittance of the dual LSC/DSSCs in the wavelengths of 400 nm to 800 nm was evaluated as 43% (**Figure 7d**). Apart from LSC-coupled DSSCs, the same group extended this strategy to

perovskite solar cells lately.[196, 197] Maximum PCEs of 7.53% and 8.99% were achieved in the upconversion-assisted dual-band and triple-band LSC-coupled perovskite solar cells, respectively.

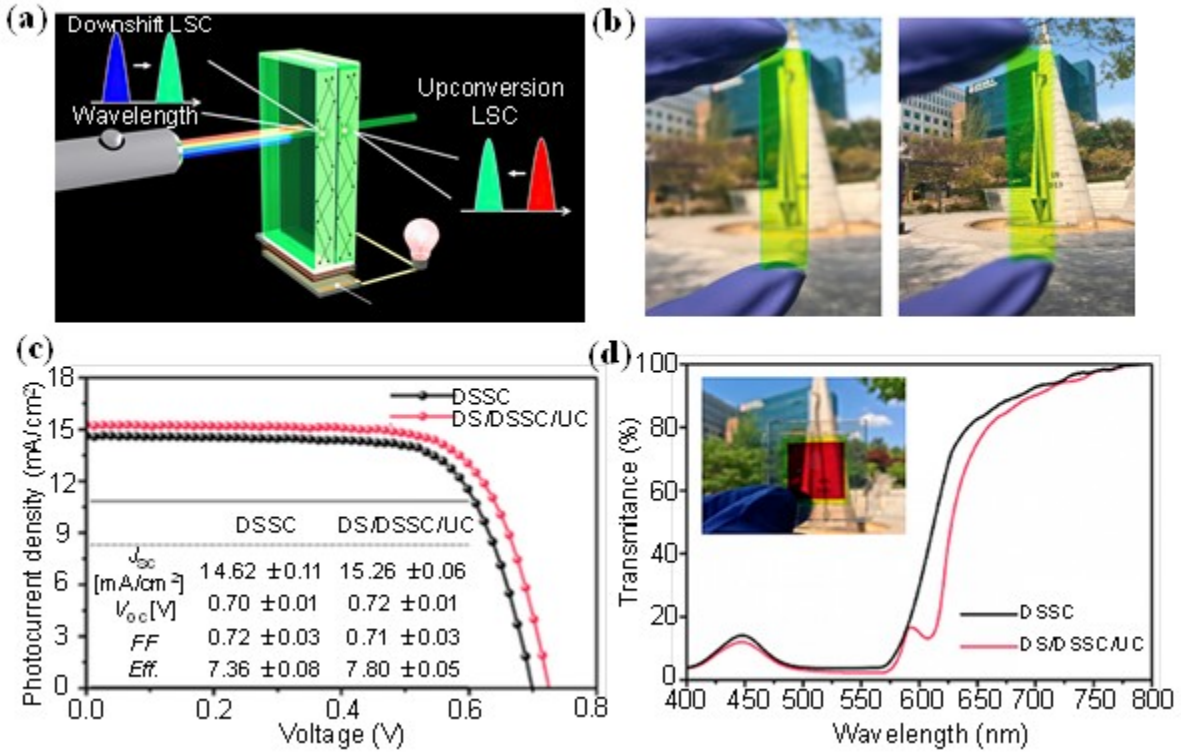

Figure 7. (a) Concept of the dual-band LSC-based solar cell system. (b) Digital images of dual-band LSC. Reproduced with permission.[194] Copyright 2016, American Chemical Society. (c) *J-V* graphs of DSSC and dual LSC/DSSC with their performances inserted. (d) Transmittance spectrum of the dual LSC/DSSC and digital photograph. Reproduced with permission.[195] Copyright 2020, American Chemical Society.

In electrically incorporated solar cells, the upconverted energy generated following light excitation and TTA is directly used for charge separation before upconversion emission.[198] In general, three approaches have been devised for harnessing TTA upconversion in DSSCs as shown in **Figure 8**. In the heterogeneous device (**Figure 8a**), the sensitizers are dissolved in the electrolyte solution while the annihilators are bonded onto the electrode surface.[199] Since the sensitizers are in the electrolyte solution, the TET from sensitizer to annihilator is still diffusion-limited, which resulted in limited upconversion efficiency. In addition, the solubility of sensitizer in the electrolyte is another problem which needs to be overcome for realizing efficient TTA upconversion.

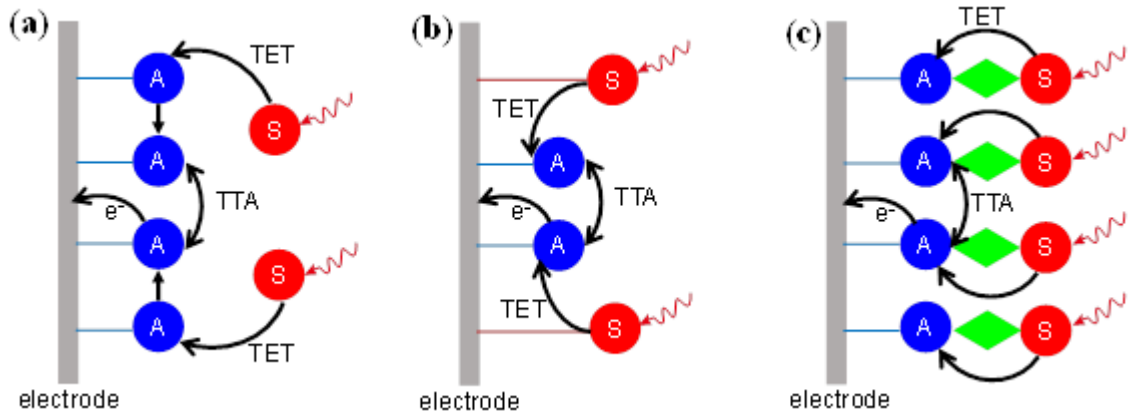

Figure 8. Schematic illustrations of (a) heterogeneous, (b) co-adsorption and (c) metal-ion-linked approaches for harnessing TTA upconversion in DSSCs.

In order to solve the triplet energy migration and sensitizer solubility issue, a co-adsorption approach was introduced (**Figure 8b**).[200] In this approach, the sensitizer and annihilator are co-adsorbed on the surface of electrode with close proximity, which improved the TET and TTA

efficiency thanks to the short distance between upconversion chromophores. A FoM of 0.036 mA cm^{-2} sun^{-2} has been achieved in a TTA upconversion integrated DSSC by co-adsorbing Pt(II)−porphyrin dye and diphenylanthracene on mesoporous TiO_2.[200] Nevertheless, this approach has the disadvantage of the relatively low light harvesting efficiency since the concentration of sensitizer on the electrode surface is limited.

Bilayer structure (**Figure 8c**) linked by metal ions has the advantages of fast TET and high surface loading concentration since the sensitizer and annihilator are linked together. In 2015, Hanson *et al.* reported a TTA upconversion integrated DSSC with self-assembling bilayers of the sensitizer and annihilator on metal oxide surface.[201] Pt(II)tetrakis(4-carboxyphenyl)porphyrin (PtTCPP) and 4,4'-(anthracene-9,10-diyl)bis(4,1-phenylene)diphosphonic acid (DPPA) were selected as sensitizer and annihilator, respectively. A 3-time enhancement of transient photocurrent was observed in TiO_2-DPPA-Zn-PtTCPP bilayer structure compared to TiO_2-PtTCPP and TiO_2-DPPA monolayers. This can be attributed to photon-to-current generation pathway provided by TTA upconversion. Lately, redox mediator, which is essential for generating the oxidized dyes and closing the circuit, was introduced into this self-assembled bilayer structure device.[202] Further photocurrent enhancement was then achieved under one sun irradiation by changing the redox mediator (**Figure 9a**).[203] The redox potential of the $Co^{2+/3+}$ mediator was found to have a significant

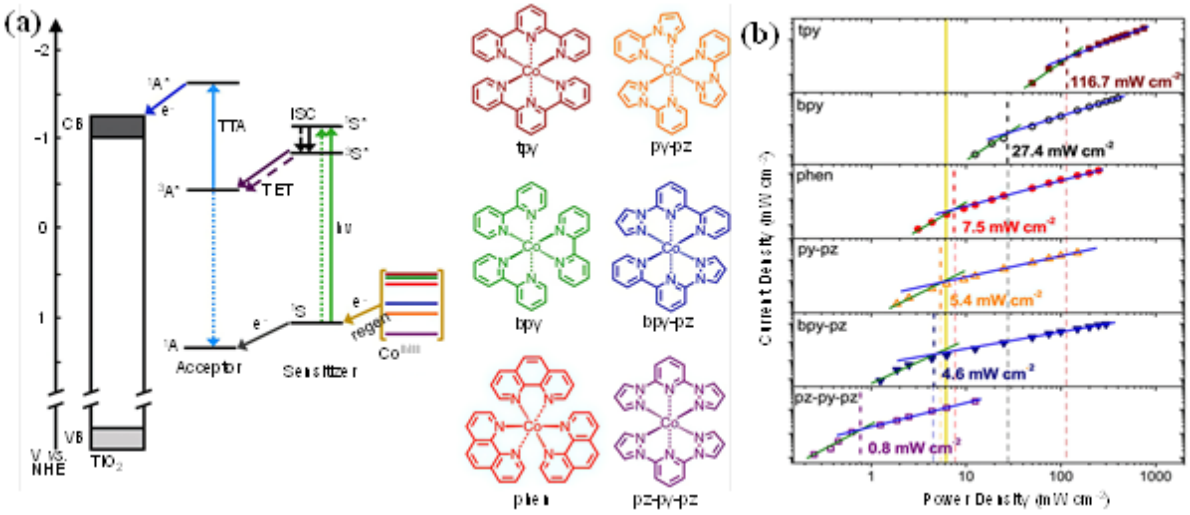

Figure 9. (a) Electronic transitions and energetics for TiO_2, Acceptor, Sensitizer, and the mediators (*vs* NHE) with the structures of the $Co^{II/III}$ redoxes. (b) Relationship between the short-circuit photocurrent density and excitation intensity at 532 nm for TiO_2-Acceptor-Zn-Sensitizer devices. Reproduced with permission.[203] Copyright 2016, American Chemical Society.

impact on the photocurrent density and I_{th}. The highest photocurrent density of 0.158 mA cm^{-2} was achieved under one sun by using CoII/III(phen)$_3$ as the mediator. And the I_{th} value of 0.8 mW cm^{-2} was obtained for CoII/III(pz-py-pz)$_2$(PF$_6$)$_2$ (**Figure 9b**). This I_{th} value is well below solar intensities as well as over hundreds times lower compared to that of CoII/III(tpy)$_2$(PF$_6$)$_2$.

The narrow absorption range of the sensitizer is another key factor limiting the TTA upconversion efficiency. To broaden sensitizers' absorption spectra, Hanson and co-workers incorporated multiple sensitizers (Pd(II) meso-tetra(4-carboxyphenyl)porphine (PdP, **Figure 5b**) and Pt(II) meso-tetra(4-carboxyphenyl)porphine (PtP, **Figure 5b**) into the TTA upconversion integrated DSSC using bilayer and trilayer self-assembly *via* metal ion linkages.[204] The multiple sensitizers in

this system work cooperatively to increase annihilator triplet excited-state densities, lower the light intensity, as well as increase overall TTA upconversion efficiency. The transmission window between sensitizer and annihilator molecules is another key factor limiting the performance of TTA upconversion integrated solar cell. A third component of singlet sensitizer (SS) was introduced into the self-assembled trilayers by the same group to harness the transmitted light.[205] A TTA upconversion photocurrent density of 0.315 mA cm^{-2} under one sun irradiation was achieved. Although SS-enhanced self-assembled trilayers strategy is promising for enhancing broad-band light absorption and improving the integrated TTA upconversion solar cell performance, cell fabrication and management involves significant complexity with four components in the photoanode (SS, sensitizer, annihilator, and TiO_2) redox mediator. Recently, NIR-to-visible upconversion system containing fluorinated zinc phthalocyanine (F16ZnPc, **Figure 5b**) as the sensitizer and perylenetetracarboxylic acid diimide (PDI-CH_3, **Figure 5a**) as the annihilator was deposited on the top of TiO_2 layer.[206] Under the NIR light (709 nm) excitation, triplets generated in F16ZnPc was efficiently transferred to PDI-CH_3. Consequently, electrons formed from the upconverted singlet excited-states of PDI-CH_3 are directly injected into TiO_2. The maximum efficiency of the absorbed photons to injected electrons in this system was 1.8%.

Apart from porphyrin derivatives used as sensitizers, QDs have been emerged as triplet sensitizers as they are relatively easy to be synthesized with small singlet-to-triplet energy gap and tunable energy levels.[207, 208] Many studies have demonstrated that localized triplets on QDs can be efficiently transferred to the organic annihilators that anchored on the QDs surface or dissolved in solution.[209-212] Recently, Hanson *et al.* reported the first example of TTA upconversion integrated solar cell using QDs as the sensitizers.[213] Although the performance is not comparable to the

previous molecular sensitized device, it showed the potential of multilayer assemblies containing QDs sensitizers in harnessing the upconversion efficiency for TTA upconversion solar cell devices.[214]

In summary, TTA based upconversion has been extensively studied both in solution and solid-state. Much progress has been made in the field of TTA upconversion in solar energy applications and the photocurrent efficiency of TTA upconversion integrated solar cells has increased considerably. However, there is still a large room to further improve the light harvesting efficiency of TTA in solar cells from different aspects including: i) improving the solid-state TTA upconversion efficiency with shifting the absorption range to NIR, ii) decreasing back energy transfer and triplet energy loss through material and device architecture design, iii) developing new mediator materials and deeply understanding the relationship between mediator molecular structure and performance, iv) incorporating TTA uponversion in more already available solar cells with outstanding efficiency.

4. OLEDs based on TTA materials

OLED devices have been successfully commercialized in many display fields thanks to the rapid development of emissive organic semiconductors from original fluorescent, to phosphorescent, TTA, TADF, and recently developed hot exciton, radicals materials.[31, 51, 52, 60, 61] The theoretical internal conversion efficiency have been increased from initial 25% to 100%. As a result, the performance of OLEDs based on organic semiconductors has been significantly improved with the highest EQE of nearly 40%.[215] Certainly, apart from the active materials, optimization of their aggregation states and device fabrication technology also play important roles for improving the performance of OLEDs, which have been well summarized in other review articles.[48, 65, 216]

Among these above-mentioned active materials, semiconductors with TTA property usually show unique blue emission with small efficiency roll-off, low operation voltage, and low cost, which are a kind of ideal materials for OELDs. Even though photoluminescence involving TTA was first evident in hydrocarbon compound solution in 1962,[66] it was not until 1998 that TTA was first proposed as a possible mechanism for a high EQE of 7.1% in OLEDs reported by Kido *et al.*[217] Much progress has been achieved in recent years for TTA-based OLEDs. In this section, recent progress of TTA-based OLEDs is systematically summarized in terms of the sensitization approaches, including charge transfer (CT)-sensitized (**4.1**) and local excited triplet-sensitized (**4.2**) TTA systems.

4.1 Charge transfer (CT)-sensitized TTA systems

Charge transfer (CT)-sensitized TTA is also known as exciplex-sensitized TTA. It is a process in which excitons are initially produced by electrical excitation on the interface between the TTA layer and its neighboring layer. Then subsequently excitons are transferred to TTA layer where singlet excited-state is formed through TTA. This singlet excited-state either decays back to the ground state to emit a photon or transfers its energy to another emissive species.[130]

In 2003, Jankus *et al.* first discovered the typical CT-sensitized TTA system in OLED device.[218] They fabricated OLEDs with a simple device structure using *N,N*'-bis(1-naphthyl)*N,N*'-diphenyl-1,1'-biphenyl-4,4'-diamine (NPB) and 1,3,5-tri(1-phenyl-1*H*-benzo[d]imidazol-2-yl)phenyl (TPBi) as the active layers. As shown in **Figure 10a**, exciplex state formed between NPB and TPBi with a triplet energy level of 2.80 eV. Consequently, triplets in exciplex state were transferred to NPB with a triplet energy level of 2.38 eV. EL spectra from OLED device was observed which was consistent with the PL spectra of NPB and NPB:TPBi films (**Figure 10b**). A majority of the EL was harvested from triplet

excitons in NPB through TTA according to the excitation-dependent PL intensity and transient EL decay experimental result, in which the slope of decayed EL changed from 0.96 to 2 in terms of the delay time (**Figure 10c**). The exciplex emission which was generated from energy transfer from NPB to the CT state of NPB/TPBi was also observed (**Figure 10d**). A maximum EQE of 2.7% was achieved, which is almost twice as high as only the direct singlets production predicts of 1.4%.

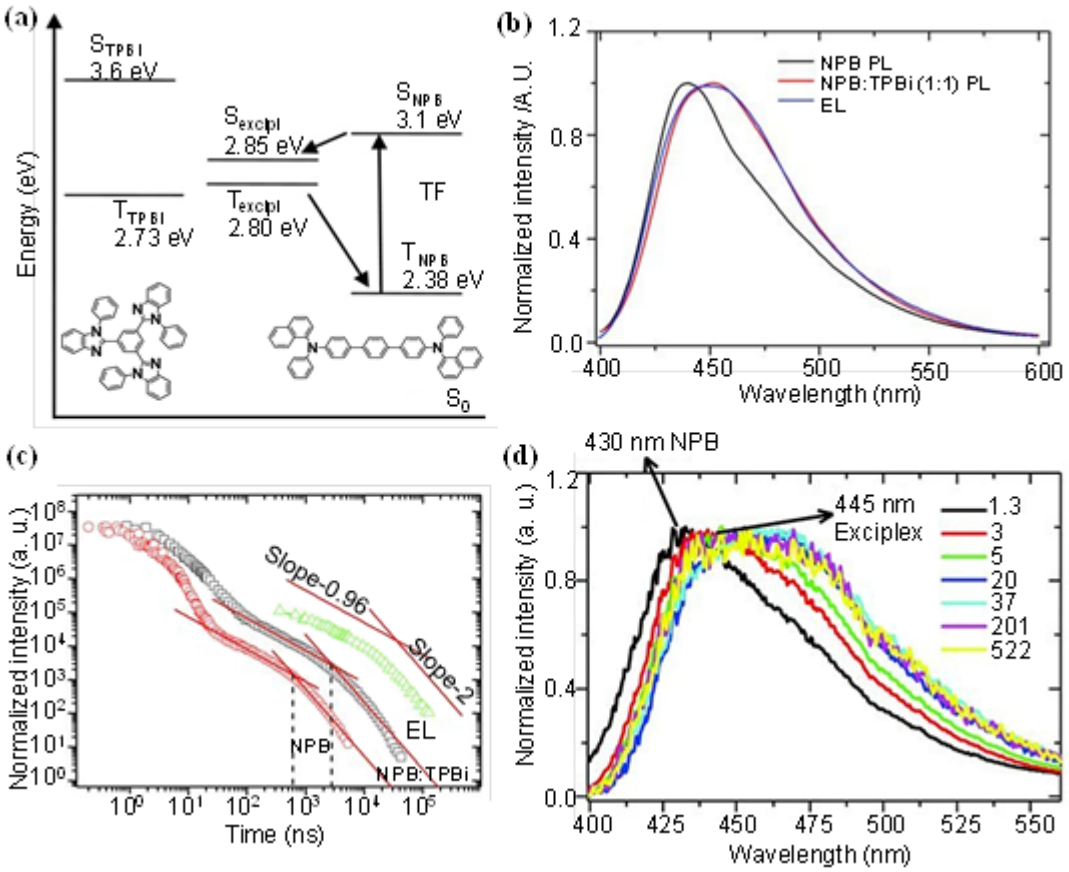

Figure 10. (a) EL spectra from the OLED device and the PL spectra of NPB and NPB:TPBi (1:1) films. (b) Energy levels and molecular structures of main materials used in CT-sensitized TTA system. (c)

Transient PL and EL decay of pure NPB and NPB:TPBi (1:1) films. (d) Time-resolved spectra from NPB:TPBi (1:1) film.[218] Copyright 2013, John Wily and Sons.

Rubrene and fullerene C_{60} are commonly used in OLEDs as annihilator/hole transporter and electron transporter, respectively.[44, 219] For instance, So *et al.* studied the origin of the EL in rubrene/C_{60} heterojunction OLEDs.[220] Comparing between devices with and without C_{60}, transient EL results revealed that the emission was mainly from rubrene through TTA process and the enhanced EL emission intensity in rubrene/C_{60} was mainly attributed to the CT states formed at the rubrene/C_{60} interface.

CT-sensitized TTA-based OLEDs usually suffer from low efficiency due to the back-energy transfer from the annihilator to the CT state. This back-energy transfer can be efficiently prevented by device modification. In 2017, Lee *et al.* fabricated a triple layer device with 4,4',4''-tris(*N*-3-methyphenyl-*N*-phenyl-amino)triphenylamine (m-MTDATA) acting as the electron donor, 1-(2,5-dimethyl-4-(1-pyrenyl)phenyl)pyrene (DMPPP) as the triplet-diffusion-singlet-blocking (TDSB) layer, and 9,10-bis(2-naphthyl) anthracene (AND) as the electron acceptor and annihilator (**Figure 11a**).[221] By introducing the TDSB layer between exciplex and TTA layers, singlet exciton diffusion and quenching was prevented. With the introduction of the TDSB layer, the EQE of blue emission OLEDs increased by 11 times to 1.1% compared to that of without TDSB layer (0.1%) (**Figure 11b**). In addition, a fluorescent dopant, 6% DPAVBi (4,4'-bis[2-(4-(*N,N*-diphenylamino) phenyl)vinyl]biphenyl) was doped into the ADN host to prevent singlet back energy transfer after TTA, and thus to improve radiative recombination efficiency. The shorter decay time of the doped TDSB OLED compared to that of TDSB offered solid evidence of the successful improvement of the radiative recombination rate. The blue EQE was improved to 3.8% (**Figure 11b**). Moreover, the exciplex emission contributed to an EQE of

1.3%, leading to a total EQE of 5.1%. This EQE was slightly higher compared to that of the conventional efficiency limit of fluorescent material-based OLEDs (5%) due to the exciplex and TTA characteristics. Recently, they used transient PL measurements to understand the origin of the improved device EQE.[222] They found that the TDSB layer contributed to the suppression of singlet quenching. However, singlet quenching by m-MTDATA/AND exciplex still existed even for the thickest TDSB layer. Therefore, there is room for improvement in CT-sensitized TTA OLEDs by such as optimizing the energy levels of the TDSB layer to further decrease the singlet quenching.

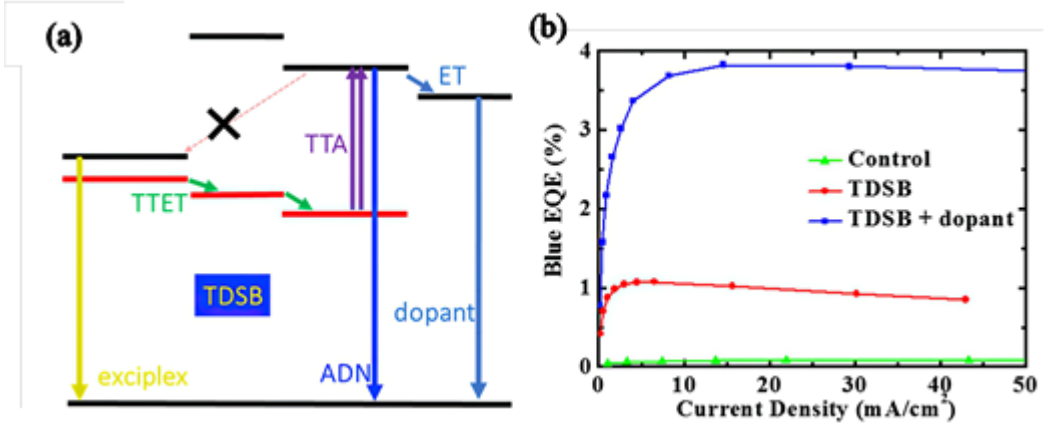

Figure 11. (a) Schematic diagram of exciton energies and transitions including TDSB and guest materials for the CT-sensitized TTA-based OLED. (b) EQE versus current density for the three CT-sensitized TTA-OLEDs.[221] Copyright 2017, American Chemical Society.

4.2 Local excited triplet-sensitized TTA systems

For local excited triplet (LET)-sensitized TTA, there are mainly two approaches to obtain triplet excitons. First, triplets are formed in a sensitizer layer and then transferred to the TTA molecules.[126]

Second, triplets are formed directly in TTA layer by charge injection.[223] Below we will discuss the realization of both of these strategies in heterojunction (4.2.1), doped (4.2.2) and non-doped (4.2.3) structures (**Figure 12**).

In the heterojunction structure (**Figure 12a**), singlet and triplet excitons are formed directly in the sensitizer layer after electron and hole recombination. The singlet excited-state in the sensitizer decays to the singlet ground state via light emission or it could intersystem cross into the triplet state depending on the nature of the sensitizer, while the triplets are transferred to the annihilator layer through TET. Consequently, upconverted singlet excitons are generated via TTA for emission. This heterojunction structure usually exhibits a dominate sensitizer emission and a weak upconverted emission from TTA, which is mainly attributed to the low TET and serious back energy transfer from annihilator to sensitizer.

Until now, TTA materials are mostly used in the doped OLED device structure as host, and/or guest (**Figure 12b**). Doping strategy has been widely used in many optoelectronic devices for integrating different excellent optical and electrical properties in one system. An EQE of above 14% has been achieved in TTA doped OLED device.[224] When TTA materials are used as host, singlet and triplet excitons are directly formed in these molecules where TTA takes places. TTA host materials usually have efficient TTA but low PL efficiency. Singlets generated in TTA host will be transferred to a more emissive guest for final EL. TTA materials with efficient TTA and high PL efficiency are normally utilized as guest. Electrogenerated triplet excitons on host materials are transferred to the TTA guest materials. Upconverted singlets generated via TTA decay radiatively for EL. Co-depositing two different TTA materials as the emissive layer is also a good alternative for constructing efficient OLED device. In this strategy, TTA may take place on both these two components. These two TTA

materials have suitable energy level where the singlet and triplet energy transfer from host to guest is energetically favorable.

For simplifying device structure and fabrication process, non-doped OLED based on neat TTA material as the emissive layer is the more practical option (**Figure 12c**). Since electron and hole recombination, TTA and light emission all take place on this single layer, it requires annihilators capable of balanced carrier mobility, efficient TTA and high PL quantum efficiency simutaneously.

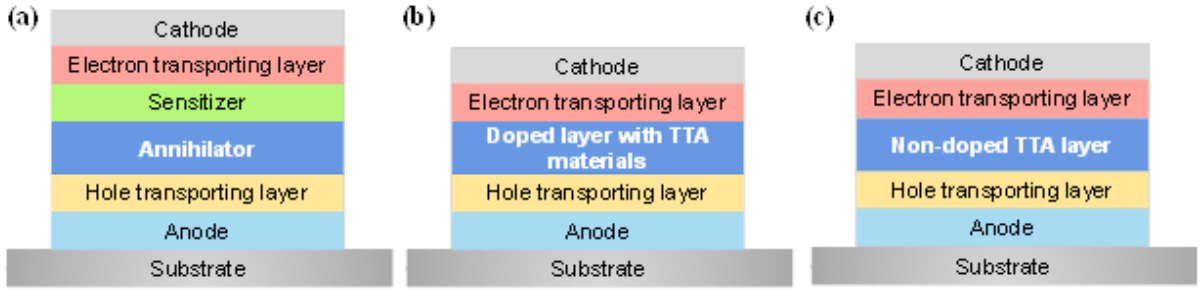

Figure 12. Schematic illustrations of (a) heterojunction, (b) doped and (c) non-doped OLED device structures based on TTA materials.

4.2.1 Heterojunction bilayer structure

Tris-(8-hydroxyquinoline)aluminum (Alq_3) is one of the most widely used electroluminescent materials in OLEDs with excellent electron transport and optical properties.[225, 226] Alq_3 is also a good candidate for sensitizer in TTA-based OLEDs. In 2018, Lee *et al.* constructed a heterojunction bilayer structure OLEDs employing Alq_3 as the sensitizer, and ADN as the blue TTA annihilator. Alq_3 has a triplet energy level of 2.0 eV which can sensitize ADN with a triplet energy level of 1.7 eV.[227]

Operation lifetime was elongated for both blue (ADN) and green (Alq_3) emission which was mainly owning to efficient utilization of excitons and separation of the recombination and emission zones. A TDSB layer with DMPPP was inserted between sensitization and emission layers to reduce the singlet quenching of blue upconverted emission from ADN by the Alq_3 with lower bandgap.[228] The overall EQE of the triple layer OLEDs was 3.07%, almost 1.5 times higher compared to that of the bilayer OLEDs.

Rubrene has been widely used in organic optoelectronic devices due to its efficient emission efficiency, strong SF, and high carrier mobility.[82, 229-231] Since the singlet energy level of rubrene is very close to the two times of its triplet energy level, both SF and TTA can occur in rubrene films.[232, 233] The conversion from SF to TTA is highly related to the distance between molecules. In 2006, Xiong *et al.* investigated the influence of intermolecular distance on the SF and TTA processes in rubrene-based OLEDs using magneto-electroluminescence (MEL).[234] A phosphorescent material, 1,3-bis(*N*-carbazolyl)benzene (mCP) was selected as the host and sensitizer. mCP has a higher triplet energy level (2.95 eV) than that of rubrene (1.20 eV), leading to effective transfer of its triplet energy to rubrene and eliminate the guest-to-host back-energy transfer. The highest efficiency of rubrene-based OLEDs was obtained with an intermolecular distance of 3.8 nm, which was attributed to the complete conversion of SF to TTA. This study provided a new approach to the efficiency improvement of rubrene-based OLEDs.

4.2.2 Doped layer structure

Apart from the above-mentioned heterojunction bilayer OLEDs structures, doping strategy is also widely used for efficient OLEDs by utilizing a TTA material as the host, and/or guest. When TTA

materials are used as host, triplet excitons can be harvested through TTA and consequently, the upconverted singlet is transferred to a more emissive guest molecule. Both internal conversion efficiency and fluorescence quantum yield can be improved in such systems. For some highly fluorescent TTA materials, they are more suitable to be used as guest to enhance the EQE of OLEDs.

4.2.2.1 TTA material as host

TTA materials usually suffer from low PL efficiency caused by aggregation induced quenching or excimer formation. Using TTA material as light-emitting host in OLEDs is an efficient approach to produce blue, green or red emissions when doped with different dopants.[28, 235-237] In this strategy, singlet and triplet excitons are formed directly in host materials where TTA takes place. Singlet excited states generated *via* TTA are transferred to the guest materials through Förster resonance energy transfer. The first efficient OLED with an EQE of 7.1% was achieved in 1988 by doping Alq_3 layer with Coumarin 6, which is an outstanding fluorescent laser dye.[217] Anthracene derivatives exhibiting high PL, EL and TTA efficiencies have been widely utilized in efficient blue fluorescent OLEDs. For instance, tetraphenylsilane (silicon-cored) anthracene derivatives (ATSA, PATSPA, NATSNA, **Figure 13a**) were synthesized by Char *et al.* in 2008 as host materials.[238] By doping with 4,4'-bis[4-(di-*p*-tolylamino)styryl]biphenyl (DPAVBi), the highest efficiency of up to 7.5 cd A^{-1} with a corresponding EQE of 6.3% was obtained in DPAVBi/PATSPA OLEDs. In 2012, Fukagawa *et al.* studied the relationship between the molecular structure of anthracene derivatives and TTA efficiency by utilizing 2,2'-bis(anthracen-9-yl)-9,9'-spirobifluorene (Spiro-FA, **Figure 13a**) and 2,2'-bis(10-phenylanthracen-9-yl)-9,9'-spirobifluorene (Spiro-FPA, **Figure 13a**) as the hosts.[239] They found that decreasing the overlap of anthracene units between adjacent molecules in the light-emitting layer is crucial for enhancing the upconversion of triplet excited-states into singlets. Efficient blue emission

OLEDs were prepared with an EQE of 7.2%. Recently, anthracene derivates-based OLEDs with an EQE of 9.2% has been fabricated by Kwon *et al.* using 9-(4-(10-phenylanthracene-9-yl) phenyl)-9*H*-carbazole (PhPC, **Figure 13a**) doped with *N,N*′-bis-dibenzofuran-4-yl-*N,N*′-bis-(2,5-dimethylphenyl)-pyrene-1,6-diamine (BPPyA) as the light-emitting layer.[131]

4.2.2.2 TTA material as guest

TTA materials with high PL efficiencies have been extensively studied as guests (dopants) in OLEDs. Cheng's group developed a series of triphenylene- and styrylpyrene-containing donor-acceptor type compounds as TTA dopant annihilators by using 2-(styryl)triphenylene (TS) as the core moiety for deep-blue emitters.[236, 240] A pyrene-containing compound, 1-(2,5-dimethyl-4-(1-pyrenyl)phenyl)pyrene (DMPPP), with a solid-state PL quantum yield (PLQY) of 85% and a singlet energy level of 3.2 eV was chosen as the host material for TS-doped OLEDs. Efficient TTA delayed fluorescence was observed through PL transient measurements in these DMPPP/TSTA (**Figure 13b**) devices with a maximum EQE of 10.2% and the maximum current efficiency of 12.3 cd A^{-1}.[236] Following this work, they developed deep-blue emitters by incorporating a styrylpyrene core and electron-donating groups. These new emitters exhibited intramolecular charge transfer emissions with high PLQY (above 85% in solution). High EQEs of 11-12% were achieved in (*E*)-*N,N*-diphenyl-4-(4-(pyren-1-yl)styryl)aniline (DPASP, **Figure 13b**)-doped devices with hosts of 4,4'-bis(*N*-carbazolyl)-1,1'-biphenyl (CBP) and DMPPP.[240] Moreover, DPASP-doped DMPPP-based OLEDs showed small efficiency roll-off, which was mainly attributed to the excellent charge balance in the emitting layer. In 2017, Kukhta *et al.* designed and synthesized new bipolar derivatives of carbazole and nitrile-substituted 1,3,5-triphenylbenzene (TPB), and studied applications in OLEDs as host-guest materials.[224] They revealed that *para*-conjugation TPB derivatives showed higher thermal

(a) **Doped systems: TTA material as host**

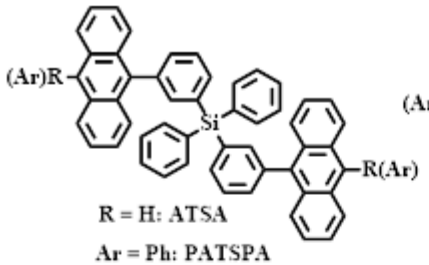

R = H: ATSA
Ar = Ph: PATSPA
Ar = 2-naphthyl: NATSNA

R = H: Spiro-FA
Ar = Ph: Spiro-FPA

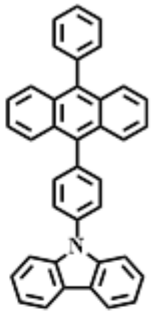

PhPC

(b) **Doped systems: TTA material as guest**

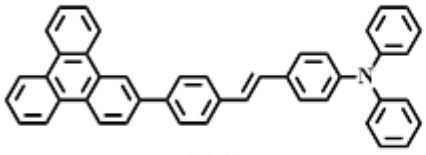

TSTA

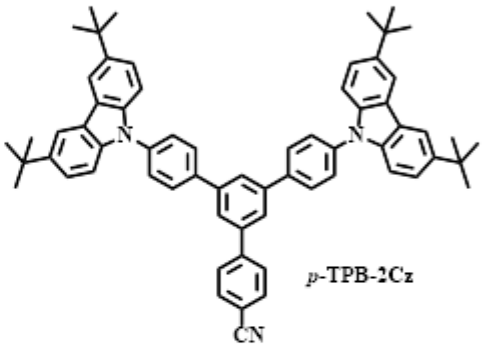

p-TPB-2Cz

BD3

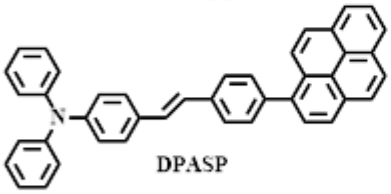

DPASP

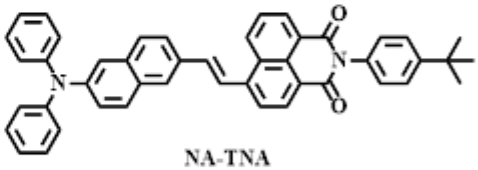

NA-TNA

(c) **Non-doped systems**

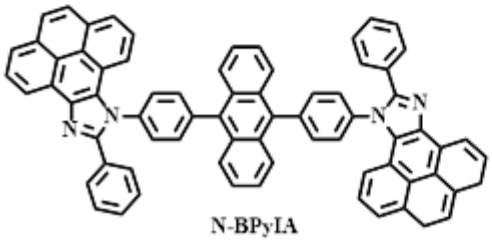

N-BPyIA

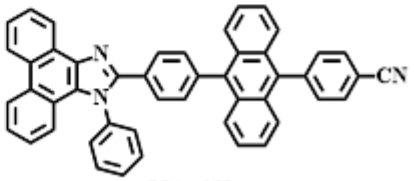

PIAnCN

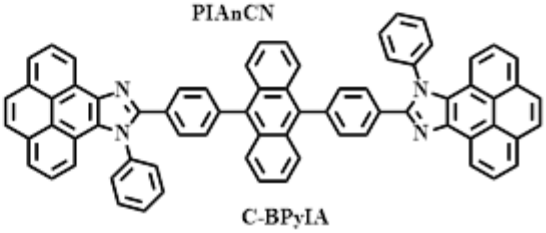

C-BPyIA

Figure 13. Chemical structures of TTA annihilators used in doped systems as (a) host, (b) guest, and (c) in non-doped systems for OLEDs.

stability, higher glass transition temperatures, lower ionization potentials, exclusively hole transport, and near-unity PL quantum efficiencies when dispersed in nonpolar media, while compounds with *meta*-linkage display ambipolar charge transport properties and high triplet energy levels. A high EQE of 14.1% was obtained in OLEDs using *p*-TPB-2Cz (**Figure 13b**) as the TTA annihilator and *m*-TPB-2Cz as an ambipolar host. The high device efficiency has been attributed to the energetically close triplet energy levels in the host and guest, enabling more efficient triplet migration and annihilation.

To provide additional benefit for triplet confinement, multicolor (deep blue, green, yellow, and red) TTA-based OLEDs (**Figure 14a**) were fabricated using 9,10-DPA, pyrene, rubrene and TIPS-pentacene (**Figure 5a**) as guests, and poly(9-vinylcarbazole) as host by Friend *et al*. in 2017.[83] Maximum EQEs of above 6% were obtained for 9,10-DPA, pyrene and rubrene-doped polymer devices (**Figure 14b**) at high doping concentrations (20%), which clearly exceeded the EQE limit (5%) of conventional fluorescent OLEDs. However, the EQEs of these devices showed a significant efficiency roll-off at the current density of 100 mA cm^{-2} which was mainly attributed to unbalanced charge injection and transport. To circumvent these issues, they developed a solution-processable inverted multilayer OLEDs (**Figure 14c**) by doping rubrene in poly (9,9'-dioctylfluorene)-co-benzothiadiazole (F8BT) as the emissive layer.[241] The delayed EL lifetime from rubrene-doped F8BT device was much longer than that of F8BT-only device, suggesting that the TTA process in rubrene-doped F8BT was more efficient than that of pure F8BT. The maximum EQE obtained from this inverted device was 6.3% with a small efficiency roll-off (**Figure 14d**). Based on the EQEs and transient EL results, the TTA-based upconversion efficiency for rubrene was calculated to be 23%,

which is almost half of the theoretical maximum value of 50%. Therefore, the TTA upconversion efficiency can be further improved by developing proper emissive annihilator molecules with high PL quantum efficiencies.

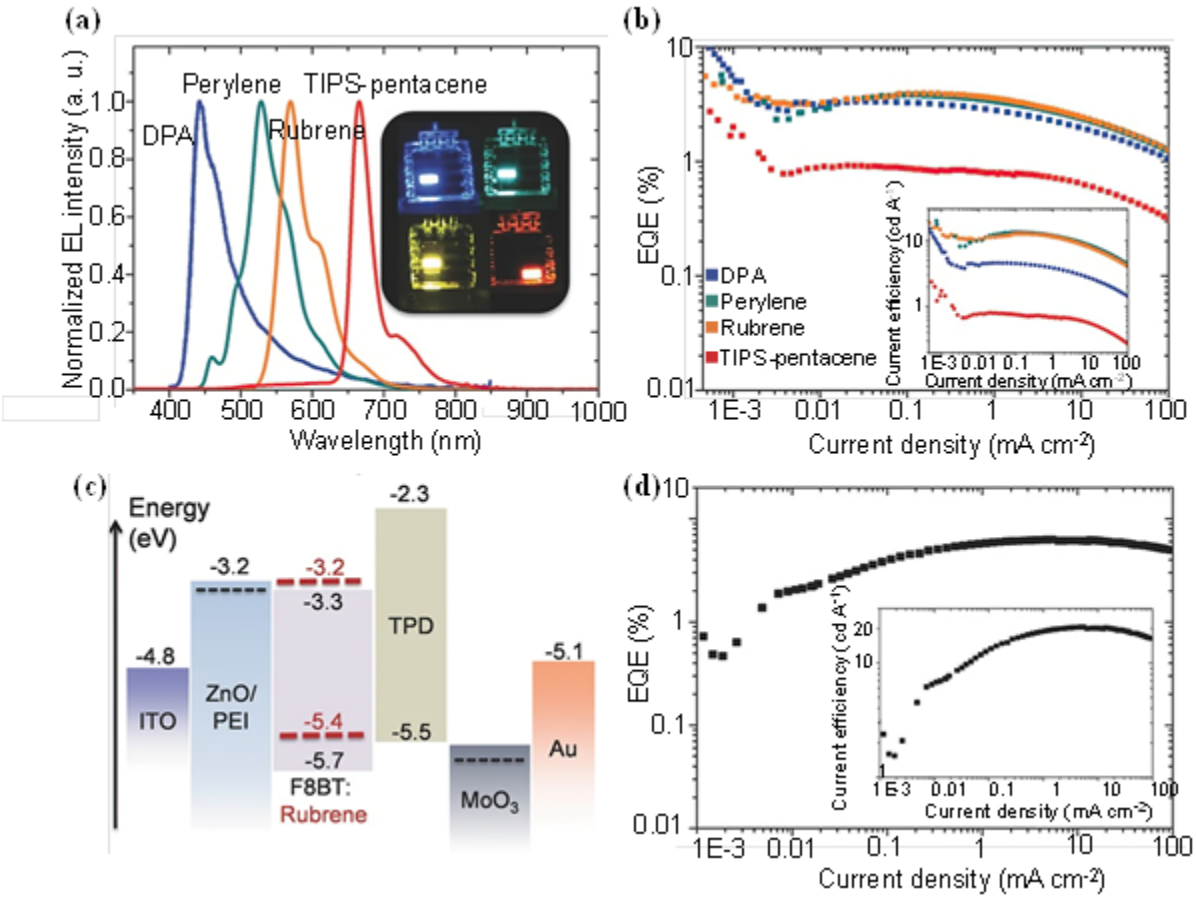

Figure 14. (a) EL spectra (insert: photographs of working devices) and (b) EQE versus current density (insert: current efficiency-current density curves) for DPA, pyrene, rubrene and TIPS-pentacene doped poly(9-vinylcarbazole)-based OLEDs. (c) Device energy level diagram and (d) EQE versus current density curve (insert: current efficiency versus current density) for inverted rubrene-doped F8BT-based OLED device. Reproduced with permission.[83] Copyright 2017, John Wily and Sons.

9,10-DPA derivatives, exhibiting high PL quantum efficiency, high electrochemical stability, and appropriate energy levels to convert triplet excited-states to singlets, have been widely used as TTA annihilators in OLEDs.[242-245] In 2014, a DA-type blue-emitting compound, 1-(10-(4-methoxyphenyl)anthracen-9-yl)-4-(10-(4-cyanophenyl)anthracene-9-yl)benzene (BD3, **Figure 13b**) was synthesized by Kido and co-workers.[246] Non-doped OLEDs based on BD3 exhibited a maximum EQE of 4.2% with a slight roll-off, which indicates the good charge balance as a result of the DA-type molecular design. Notably, their doped devices (BD3 in CBP) exhibited a high EQE of >10% with Commission Internationale de l'Éclairage (CIE) coordinates of (0.15, 0.06), which is close to the CIE of the high-definition television standard blue (0.14, 0.08).[247]

4.2.2.3 TTA material as hosts and guests

Incorporating two TTA materials together as the emissive layer is another alternative approach to improve the efficiency of OLEDs. Recently, molecules with intramolecular CT feature were reported displaying TTA character.[237, 248] Lu and co-workers found a CT-featured naphthalimide derivative (CzPhONI) with a quite small exchange energy but a lower lying $^3\pi\pi^*$ state than the ^{3}CT state, which is capable of harvesting triplets through TTA.[249] Another naphthalimide compound (*E*)-2-(4-(tbutyl)phenyl)-6-(2-(6-(diphenylamino)naphthalen-2-yl)vinyl)-1*H*-benzo[*de*]isoquinoline-1,3(2*H*)-dione (NA-TNA, **Figure 13b**) with intramolecular CT character was exploited by the same group, by using diphenylamine, vinylnaphthalene and 1,8-naphthalimide as the electron donor (D), π-bridge and electron acceptor (A), respectively.[250] Efficient host/guest energy transfer pair was formed in both CzPhONI and NA-TNA materials. They proposed that TTA may happen in both host and guest material for harvesting triplet excitons. Singlets generated in host CzPhONI was transferred to NA-TNA (guest) for final EL. OLEDs based on NA-TNA-doped-CzPhONI (in 6 wt%) showed a maximum

EQE of 5.8% (12 cd cm^{-2}), a maximum current efficiency of 7.73 cd A^{-1}, and maximum brightness of 31940 cd m^{-2}.

4.2.3 Non-doped layer OLEDs

In heterojunction and doped structures, strict energy requirements often result in complex manufacture process and parasitic energy loss. To circumvent these issues, non-doped OLED based on neat TTA material as the emissive layer is the more practical option for simplifying device structure and fabrication process. Recently, some non-doped OLEDs based on blue TTA materials have been reported.[251-253] Anthracene and pyrene (typical classes of blue light-emitting materials), and a variety of derivatives combined different side groups at different positions have been reported.[243, 254-256] In 2018, Lu *et al.* synthesized a blue-emitting material, PIAnCN (**Figure 13c**) by connecting phenanthroimidazole (PI) with a cyano substituted anthracene (AnCN).[251] A maximum EQE of 9.4% of the non-doped OLEDs was achieved at high luminescence of 1000 cd m^{-2}. Additionally, the negligible EQE roll-off was observed (*e.g.*, 8.1% at 10 000 cd m^{-2}). Lately, the same group combined two pyreno[4,5-d]imidazole moieties with an anthracene core to reduce non-radiative transitions of molecules. High PL quantum efficiencies in two new synthesized materials (N-BPyIA and C-BPyIA, **Figure 13c**) were achieved. Non-doped OLEDs based on N-BPyIA showed sky blue emission with CIE coordinates of (0.22, 0.31), with a EQE of 5.6% and a low efficiency roll-off.[252] By replacing the substituent to carbazole, Wang *et al.* synthesized TTA emitter molecule, 4-(10-(9-phenyl-9*H*-carbazol-3-yl)-anthracen-9-yl)benzonitrile (3CzAnBzt).[253] OLEDs based on non-doped 3CzAnBzt exhibited a maximum EQE of 10.1%, which is among the highest efficiencies of non-doped devices so far.

In summary, TTA materials with efficient upconversion property show a promising route to harvest triplet excitons and decrease efficiency roll-off in OLEDs. Different approaches including CT-sensitized TTA and LET-sensitized TTA were developed to give efficient OLEDs. Considering the practical application of TTA materials in OLEDs, non-doped TTA systems are desirable owing to its simplified device fabrication process. However, to date, materials with high PL quantum efficiency and efficient TTA process are still very rare and require further development. In addition, most TTA-based OLEDs have been limited to blue or deep blue emission. Hence, diversifying the TTA materials with different emission color is necessary for further expanding the application in OLEDs.

5. OLETs based on TTA materials

The unique integrated device architecture of OLETs provides an ideal platform for studying the fundamental optoelectronic properties of organic semiconductors, such as charge injection, carrier transport, hole and electron recombination, and exciton formation processes. Owning to the compact device architecture, OLETs hold great potentials in integrated electronics, smart display, electrically pumped lasers, *etc*.[20, 21, 257-266] Active semiconductor materials to give efficient OLET device performance should exhibit both a high charge carrier mobility and a high PL quantum efficiency. However, these two properties are often a trade-off and not readily observed in single material. For instance, materials with a high carrier mobility usually exhibit efficient π-π stacking. The strong π-π stacking often results in fluorescence quenching due to the formation of non-radiative decay routes, such as exciplexes, excimers, and charge transfer states, *etc*. Therefore, it is

highly challenging to integrate properties of high carrier mobility and strong luminescence in one molecule efficiently. The serious lack of such high mobility emissive materials has greatly restricted the development of OLET devices and their applications in the fields. Similar to OLED devices, bilayer and multilayer OLETs have also been developed and investigated over the past years. From the aspects of simplifying the device architecture for low-cost fabrication and maximizing reduction of the optical loss induced by multilayer for higher efficiencies, single-layer OLETs are promising for potential applications in display, electrically-pumped lasering as well as other integrated optoelectronic devices and circuits.[267] In recent years, the emergence of some high mobility luminescent materials has accelerated the development of OLETs field.[4, 268-278] However, materials currently used in OLETs have been mainly based on fluorescent materials, which can only utilize 25% singlet excitons, while 75% triplet excitons are wasted. Lately, both phosphorescent and TADF emitters have been utilized for the construction of multiple-layer OLETs, and the maximum EQE of up to 9.0% has been achieved.[58, 59, 63, 64, 279-281] However, current efficient TADF molecules are hard to integrate both high mobility and efficient PLQY due to their own steric molecular structure nature in material design.

In contrast, organic semiconductors capable of TTA is promising for OLETs due to their intrinsic advantages compared to other triplet harvesting materials, such as TADF and phosphorescent materials. They also feature below advantages: i) TTA-based emission materials have relatively short lifetime which provide better operational stability especially for blue light-emitting devices despite lower internal conversion efficiency, compared to TADF and phosphorescent materials. ii) The conjugated molecular structures and the large transition dipole moment of TTA molecules make them easier to realize high carrier mobility and efficient radiative decay rate as well as high light out-

coupling efficiency, which is hard for TADF molecules due to the steric encumbrance nature of the molecular structures. ii) TTA-based molecules are relatively easy to prepare with low-cost compared to phosphorescent materials, since most of the efficient phosphorescent materials contain rare heavy metals.

The maximum exciton utilization efficiency can be improved from 25% to 62.5% using TTA materials. To date, less attention has been paid into the application of TTA materials in OLETs. In 2015, Pandy *et al.* first investigated the influence of TTA on overall efficiency of light emission using a heterojunction OLET (**Figure 15a**) that were composed of rubrene and rubrene/C_{60}, respectively.[282] The presence of C_{60} with rubrene lead to higher EQE than the control device of poly(2,5-bis(3-hexadecylthiophen-2-yl)thieno[3,2-b]thiophene (PBTTT)/rubrene (**Figure 15b**). PBTTT/rubrene OLET with C_{60} exhibited better electrical and optical output characteristics compared to the device without C_{60} (**Figure 15c** and **15d)**. The relevant energy level diagram (**Figure 15e**) and operation mechanism of PBTTT/rubrene OLET with C_{60} (**Figure 15f**) revealed that charges were injected into the C60 layer, and the CT excitons formed in C60 subsequently transferred to rubrene. Efficient light emission attributed to TTA in rubrene accroding to the ultrafast spectral results.

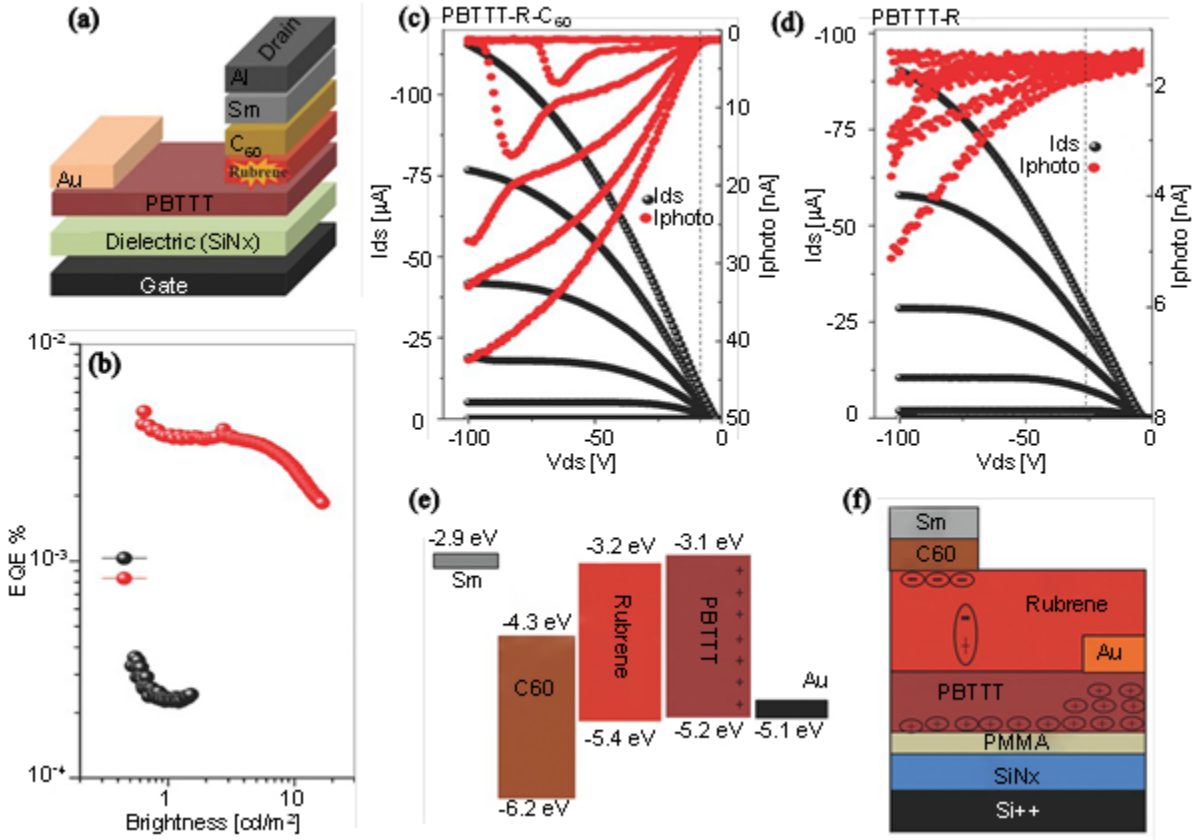

Figure 15. (a) p-type OLET device structure with a layer of C_{60}. (b) EQE vs brightness of OLETs where OLET with C_{60} shows an order of higher magnitude EQE than the control OLET. Output and optical characteristics of (c) PBTTT/rubrene/C_{60} and (d) PBTTT/rubrene OLETs. (e) Schematics of HOMO-LUMO based energy level diagram of the multilayer OLET structures. (f) Charge injection and transport mechanism effective in OLET operation of PBTTT/rubrene/C_{60}. Reproduced with permission.[282] Copyright 2017, John Wily and Sons.

In 2019, Tanigaki *et al.* fabricated a bilayer OLET composed of a tetracene crystal as a carrier transporter and a 4-(dicyanomethylene)-2-methyl-6-(p-dimethylaminostyryl)-4*H*-pyran (DCM1)-doped tetracene crystal as a light emitter.[75] Tetracene single crystal was chosen for the transport

layer, considering the high carrier mobility.[283] Additionally, tetracene shows excellent singlet fission property, which is a process by which a singlet exciton can be converted into two triplet excitons.[43, 45, 284, 285] More than 99% of singlet fission efficiency was estimated in a tetracene thin film.[286] DCM1 molecules with a smaller HOMO-LUMO energy gap compared to that of tetracene was employed as the dopant, which also exhibit TTA property. The bilayer OFET devices showed ambipolar behaviour with a hole transport mobility of 3.17 $cm^2 V^{-1} s^{-1}$ and an electron transport mobility of 0.99 $cm^2 V^{-1} s^{-1}$. In the bilayer OLETs, excitons were generated by a carrier recombination process in the bottom of the bottom tetracene crystal. Triplets formed from carrier recombination and singlet fission diffused to the top DCM1-doped tetracene layer. It was proposed that triplet energy in tetracene were transfer to DCM1, and TTA-based delayed fluorescence emission was observed from DCM1. However, it is a pity that more solid evidence was lacked in this work to support the occurrence of TTA process in DCM1 molecules.

Organic semiconductor materials capable of high mobility and TTA with high fluorescent efficiency is significant to facilitate the improvement of OLETs. Meanwhile, it is meaningful to expand OLETs' application to related areas, such as electronically pumped organic lasers, photonic communications, integrated electronics, *etc*. However, to date, the development of high mobility TTA materials is still at a primitive stage. Therefore, more efforts need to be put to this field from different aspects. Three proposed approaches are provided here, including design and synthesis of new high mobility TTA materials, development of high mobility TTA systems by doping TTA molecules into high mobility matrix, and improvement of TTA rate and efficiency.

As mentioned earlier, anthracene derivatives are widely used as annihilators for TTA. Meanwhile, high mobility and strong PL emission have been successfully integrated in many anthracene

derivatives, such as 2,6-diphenylanthracene (2,6-DPA) and 2,6-di(2-naphthyl)anthracene (dNaAnt).[4, 269, 270, 274-278, 287-289] Thus, several questions raised here: is it possible to realize TTA in these high mobility emissive anthracene derivatives? How high their TTA efficiency would be? Additionally, are other high mobility emissive polycyclic aromatic hydrocarbon molecules (*e.g.*, pyrene derivatives, perylene derivatives and fluorene derivatives) possible to exhibit efficient TTA as well?[272, 273, 290] To answer these questions, it is essential to have a systematic study on these materials, which is significantly important to understand the exciton interaction mechanism in these materials. Moreover, to date, most work in the field has focused on the search of high mobility or efficient TTA materials based on polycyclic aromatic hydrocarbon molecules (such as acenes), but very little work has been done in the development of new molecular families. Therefore, there is an urgent need for exploring new classes of high mobility TTA materials.

Molecular doping strategy has been intensively applied in the optoelectronic field to allow tuning the electrical and optical properties for organic semiconductors.[291-295] Apart from the strategy of directly exploring high mobility emissive molecules, molecular doping provides a more operationally convenient way to integrate carrier mobility and PL emission into one system. Therefore, doping TTA molecules into high mobility matrix is supposed to be an excellent approach to harvest triplet excitons for OLETs materials. Appropriate molecule pairs are required to be selected with suitable energy level to allow the triplet excitons generated in high mobility molecules can be efficiently transferred to the TTA molecules, where triplet excitons can be harvested through TTA process. In this approach, carrier mobility might be sacrificed at some extent due to the doping of TTA molecules. Thus, how to find the balance between the carrier mobility and triplet exciton harvesting efficiency is the key to realize efficient OLETs material systems.

One of the initial motivations for OLETs is the electronically pumped organic lasers, which require materials with high PL quantum efficiency, balanced bipolar carrier transportability and no spectral overlap between lasing wavelength and excited-state and polaron absorptions, as well as the effective management of fast triplet accumulation under electrical excitation.[23] Currently, the materials used for organic laser are mostly fluorescent, which can only utilize singlet exciton after charge recombination. Therefore, it is urgent to develop materials that are capable of harvesting triplets efficiently. To date, TADF and phosphorescent molecules with amplified spontaneous emission (ASE) property have been reported.[296-298] However, less attention has been paid to TTA-based organic laser materials. TTA materials are promising for use in electrically pumped organic lasers due to their intrinsic merits such as effective management of fast triplet accumulation, high EQE, short radiative decay lifetime and high carrier mobility compared to conventional fluorescent materials.[299, 300] For electrically pumped lasing, ultrafast upconversion of triplet excitons to singlet is necessary.[301] Therefore, more efforts need to be made in this area to realize high mobility TTA materials with good laser property.

Integration of high carrier mobility and efficient TTA in one molecule is not only essential to increase the internal quantum efficiency of OLETs but also important to simplify the OLETs device architecture, which can provide a more convenient and accurate way to study the fundamental optoelectronic properties of organic semiconductors. Meanwhile, the development of high mobility TTA-based laser materials is important to expand the application of OLETs to electrically pumped organic lasers. Currently, some explorations have been carried out in our group and the preliminary results have confirmed the above assumptions, which will contribute to the integration of high mobility and efficient exciton utilization in an organic semiconductor for significantly improving the

electroluminescence efficiency in OLETs. For instance, recently, we have systematically studied the TTA property of 2,6-DPA, one of the most representative high mobility emissive organic semiconductors reported in our group.[4, 269, 278, 302] In this study, PtOEP was selected as the sensitizer due to its appropriate triplet energy level (1.93 eV), compared to that (1.63 eV) of 2,6-DPA. Clearly, under excitation at 532 nm, bright blue upconverted emission was acquired from both PtOEP/2,6-DPA dilute solution and thin film (**Figure 16a** and **16b**). In addition, a double logarithmic plot of integrated upconverted emission as a function of excitation power density in PtOEP/2,6-DPA films was obtained (**Figure 16c**), which further confirmed the possibility of integrating high carrier mobility, strong emission and high triplet exciton utilization efficiency in one molecule. Furthermore, based on the consideration of better utilization and regulation of the triplet excitons in 2,6-DPA, a highly emissive lasing material was doped into 2,6-DPA. Singlets generated in host 2,6-DPA *via* TTA can be efficiently transferred to the guest molecule to give higher PL quantum efficiency and even lasing character based on the property of doped material (**Figure 16d**). The 2,6-DPA only and molecular doped system-based single layer OLETs are highly emissive under low voltage (**Figure 16e** and **16f**). Deeper investigation and improvements are still under way.[296] This observation of TTA property in high mobility emissive 2,6-DPA semiconductor provides a promising way for the improvement of PL quantum efficiency, and triplet exciton utilization efficiency, as well as emission characters (emission colors, lasing, *etc*). This approach could

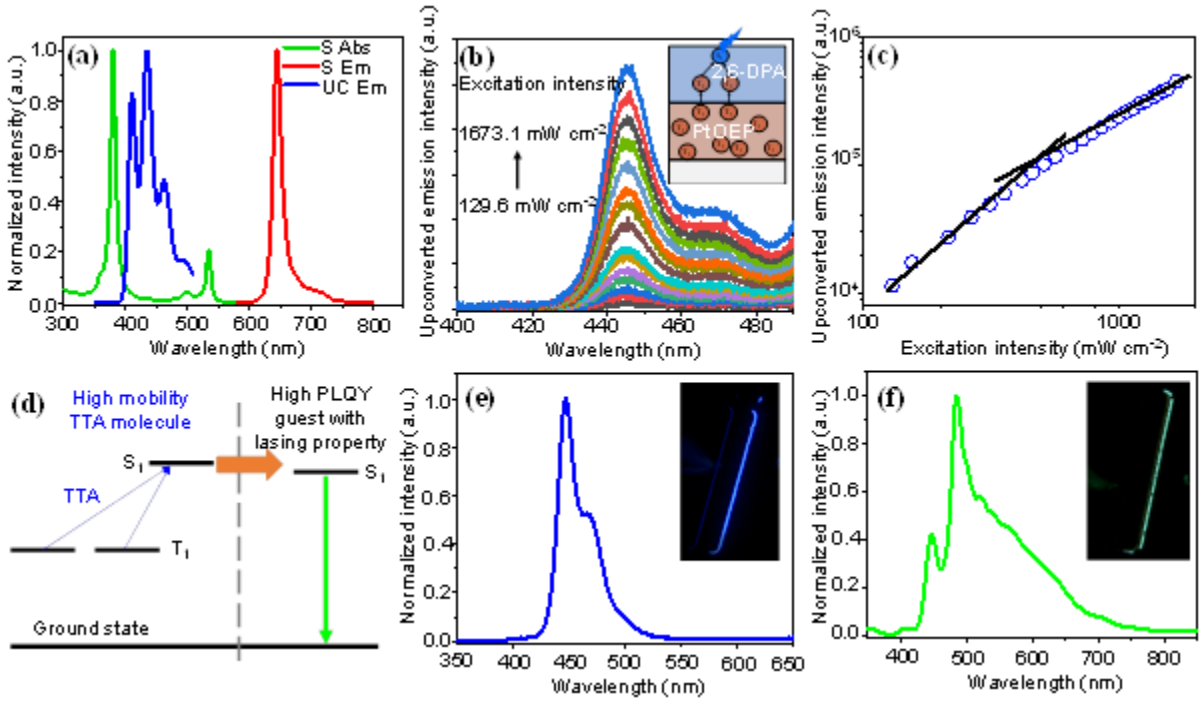

Figure 16. (a) Absorption and emission spectra of PtOEP, and upconverted emission spectra of 2,6-DPA in dilute THF solution. (b) Upconverted emission spectra of 2,6-DPA films as a function of excitation intensity. (c) A double logarithmic plot of integrated upconverted (UC) emission dependence on excitation power density in PtOEP/2,6-DPA thin film. (d) Illustration of the concept to realize high mobility emissive semiconductor system with high triplet utilization efficiency. EL spectra and images of (e) 2,6-DPA only-based single layer OLET and (f) laser material-doped 2,6-DPA based single layer OLET.

also be extended to other high mobility emissive organic semiconductors and stimulate other related investigations from material science to device physics in this field.

6. Conclusion and perspectives

Efficiency of optoelectronic devices can be boosted by harvesting sub-bandgap photons and triplet excitons. TTA upconvesion, an efficient approach of converting two triplet excitons to one singlet exciton, has been widely studied and applied to improve the efficiency of photovoltaics, OLEDs, and OLETs due to its intrinsic advantages.

This review summarized and discussed the development concerning TTA materials and their applications in optoelectronic devices. Successful examples have demonstrated that TTA upconversion is a promising strategy to harvest sub-bandgap photons and triplet excitons. Although significant progress has been made in these areas, more efforts are still required to improve the efficiency of TTA upconversion and its optoelectronic devices from different aspects.

First, the selection of active chromophore needs to be diversified. To date, in optically excited TTA upconversion systems, a large number of sensitizers and annihilators have been developed for TTA upconversion in different spectral ranges with various efficiencies. However, most of the sensitizers are still limited to Pt or Pd porphyrin derivatives, while the annihilators are mostly limited in polycyclic aromatic hydrocarbons. Even though some new classes of annihilators have been reported recently, the TTA upconversion efficiency still needs to be further improved.[236, 303] In addition, sensitizers with high molar absorptivities in the red/NIR range are desired to harvest sunlight in TTA upconversion integrated soalr cell devices. In electrically excited TTA upconversion systems, more annihilators with high TTA efficiency and high PL quantum efficiency are expected for constructing non-doped OLEDs to simplify the fabrication process. In addition, more annihilators with standard blue emission and narrow full width at half maximum are required for promoting the application in industry.

Second, energy loss in TTA upconversion-based organic optoelectronic devices is detrimental for the overall efficiency. In TTA upconversion integrated photovoltaics, back energy transfer from annihilator to sensitizer dramatically reduced the upconverted emission intensity. To block this energy loss channel, optimizing the chromophore concentration and the distance between the sensitizer and annihilator is a good option. TTA-based OLEDs also face energy loss issue which is caused by strict energy requirements and complicated device structure. This energy loss is possible to be avoided by managing the energy alignment of annihilators and optimizing device structures. For example, inserting a TDSB layer between sensitization and emission layers has been proved as an efficient approach.[221, 222]

Third, harvesting triplet excitons in OLETs is of significance to improve the EQE and promote their applications in other related areas, especially the injecting lasing. The utilization of TTA materials in OLETs is far legging behind other materials (TADF and phosphorescent materials) with high triplet exciton harvesting efficiency. Thanks to the conjugated molecular structures and the large transition dipole moment of TTA molecules, it is more promising to realize high mobilities and high exciton harvesting efficiencies in one molecule. Developing new semiconductor molecules with integration of high mobility and efficient TTA is not only important to enrich the OLETs active material family but also essential to harvest triplet excitons. In this case, simplified OLETs architecture can be fabricated based on the high mobility TTA materials with a high exciton harvesting efficiency and small efficiency roll-off. Moreover, to facilitate the application of TTA-based lasers in the future, it is essential to increase the TTA rate, reduce the spectral overlap between photoluminescence wavelengths and excited-state absorption to realize the laser oscillation property.

Overall, through the comprehenssive sumamrization and discussion, this review hopes to provide valuable guidelines for future related research and advancement in organic optoelectronics by rationally utilizing the triplet excitons in organic semiconductors.

Acknowledgements

This work was supported by the Ministry of Science and Technology of China (2017YFA0204503, 2018YFA0703200), Natural Science Foundation of China (61890943, 51725304, 91833306, 22021002, 51733004,), the. International Cooperation Program of Chinese Academy of Sciences (GJTD-2020-02, 121111KYSB20200004), the Youth Innovation Promotion Association of the Chinese Academy of Sciences, the National Program for Support of Top-notch Young Professionals, and Beijing National Laboratory for Molecular Sciences (BNLMS-CXXM-202012). WWHW acknowledges the support from the Australian Research Council through the ARC Centre of Excellence in Exciton Science (CE170100026). SCL and EBN would like to thank the Australian Research Council (ARC DP200103036). C. Gao acknowledges Prof. Qian Peng from School of Chemical Sciences, University of Chinese Academy of Sciences, Beijing, China for useful discussions.

Received: ((will be filled in by the editorial staff))

Revised: ((will be filled in by the editorial staff))

Published online: ((will be filled in by the editorial staff))

References

[1] A. J. Heeger, *Rev. Mod. Phys.* **2001**, *73*, 681.

[2] A. C. Siegel, S. T. Phillips, M. D. Dickey, N. Lu, Z. Suo, G. M. Whitesides, *Adv. Funct. Mater.* **2010**, *20*, 28.

[3] H. Dong, X. Fu, J. Liu, Z. Wang, W. Hu, *Adv. Mater.* **2013**, *25*, 6158.

[4] X. Zhang, H. Dong, W. Hu, *Adv. Mater.* **2018**, *30*, 1801048.

[5] S. Fratini, M. Nikolka, A. Salleo, G. Schweicher, H. Sirringhaus, *Nat. Mater.* **2020**, *19*, 491.

[6] Z. Ni, H. Wang, H. Dong, Y. Dang, Q. Zhao, X. Zhang, W. Hu, *Nat. Chem.* **2019**, *11*, 271.

[7] Y. Zhang, W. Hu, *Sci. China, Ser. B: Chem.* **2009**, *52*, 751.

[8] P. Wang, D. Liu, Y. Wang, P. Zhang, P. Yu, M. Wang, Y. Zhen, H. Dong, W. Hu, *Chin. Chem. Lett.* **2020**, *31*, 2909.

[9] Z. Qin, C. Gao, W. W. H. Wong, M. K. Riede, T. Wang, H. Dong, Y. Zhen, W. Hu, *J. Mater. Chem. C* **2020**, *8*, 14996.

[10] K. Zhou, K. Dai, C. Liu, C. Shen, *SmartMat* **2020**, *DOI: 10.1002/smm2.1010*.

[11] Y. Yao, Y. Chen, H. Wang, P. Samorì, *SmartMat* **2020**, *DOI: 10.1002/smm2.1009*.

[12] C. W. Tang, *Appl. Phys. Lett.* **1986**, *48*, 183.

[13] L. Meng, Y. Zhang, X. Wan, C. Li, X. Zhang, Y. Wang, X. Ke, Z. Xiao, L. Ding, R. Xia, *Science* **2018**, *361*, 1094.

[14] Y. Cui, H. Yao, T. Zhang, L. Hong, B. Gao, K. Xian, J. Qin, J. Hou, *Adv. Mater.* **2019**, *31*, 1904512.

[15] S. Li, C.-Z. Li, M. Shi, H. Chen, *ACS Energy Lett.* **2020**, *5*, 1554.

[16] J. Yang, Z. Zhao, S. Wang, Y. Guo, Y. Liu, *Chem* **2018**, *4*, 2748.

[17] G. Osbourn, J. Schirber, T. Drummond, L. Dawson, B. Doyle, I. Fritz, *Appl. Phys. Lett.* **1986**, *49*, 731.

[18] B. H. Lee, B. B. Hsu, S. N. Patel, J. Labram, C. Luo, G. C. Bazan, A. J. Heeger, *Nano Lett.* **2016**, *16*, 314.

[19] C. Zhang, P. Chen, W. Hu, *Small* **2016**, *12*, 1252.

[20] C.-F. Liu, X. Liu, W.-Y. Lai, W. Huang, *Adv. Mater.* **2018**, *30*, 1802466.

[21] M. U. Chaudhry, K. Muhieddine, R. Wawrzinek, J. Sobus, K. Tandy, S. C. Lo, E. B. Namdas, *Adv. Funct. Mater.* **2019**, *30*, 1905282.

[22] A. S. Sandanayaka, T. Matsushima, F. Bencheikh, S. Terakawa, W. J. Potscavage Jr, C. Qin, T. Fujihara, K. Goushi, J.-C. Ribierre, C. Adachi, *Appl. Phys. Express* **2019**, *12*, 061010.

[23] C. Adachi, A. S. D. Sandanayaka, *CCS Chem.* **2020**, *2*, 1203.

[24] F. Cicoira, C. Santato, *Adv. Funct. Mater.* **2007**, *17*, 3421.

[25] H. Gao, J. Liu, Z. Qin, T. Wang, C. Gao, H. Dong, W. Hu, *Nanoscale* **2020**, *12*, 18371.

[26] A. Hashimoto, *Nature* **1990**, *347*, 53.

[27] W. Helfrich, W. Schneider, *Phys. Rev. Lett.* **1965**, *14*, 229.

[28] A. Köhler, H. Bässler, *Mater. Sci. Eng. R Rep.* **2009**, *66*, 71.

[29] S. Guo, S. Liu, K. Y. Zhang, W. Huang, Q. Zhao, *J. Semicond.* **2019**, *40*, 070402.

[30] Y. V. Romanovskii, A. Gerhard, B. Schweitzer, U. Scherf, R. Personov, H. Bässler, *Phys. Rev. Lett.* **2000**, *84*, 1027.

[31] M. A. Baldo, D. O'brien, Y. You, A. Shoustikov, S. Sibley, M. E. Thompson, S. R. Forrest, *Nature* **1998**, *395*, 151.

[32] Z. Zhou, C. Qiao, K. Wang, L. Wang, J. Liang, Q. Peng, Z. Wei, H. Dong, C. Zhang, Z. Shuai, *Angew. Chem. Int. Ed.* **2020**, *59*, 21677.

[33] S. Hirata, *Adv. Opt. Mater.* **2017**, *5*, 1700116.

[34] S. Mukherjee, P. Thilagar, *Chem. Comm.* **2015**, *51*, 10988.

[35] W. Zhao, Z. He, B. Z. Tang, *Nat. Rev. Mater.* **2020**.

[36] Q. Li, Y. Tang, W. Hu, Z. Li, *Small* **2018**, *14*, 1801560.

[37] Y.-N. Liu, S.-F. Wang, Y.-T. Tao, W. Huang, *Chin. Chem. Lett.* **2016**, *27*, 1250.

[38] B. T. Luppi, D. Majak, M. Gupta, E. Rivard, K. Shankar, *J. Mater. Chem. A* **2019**, *7*, 2445.

[39] R. Chen, Y. Tang, Y. Wan, T. Chen, C. Zheng, Y. Qi, Y. Cheng, W. Huang, *Sci. Rep.* **2017**, *7*, 6225.

[40] T. F. Schulze, T. W. Schmidt, *Energy Environ. Sci.* **2015**, *8*, 103.

[41] M. J. Tayebjee, A. A. Gray-Weale, T. W. Schmidt, *J. Phys. Chem. Lett.* **2012**, *3*, 2749.

[42] W. Shockley, H. J. Queisser, *J. Appl. Phys.* **1961**, *32*, 510.

[43] M. B. Smith, J. Michl, *Chem. Rev.* **2010**, *110*, 6891.

[44] A. K. Pandey, *Sci. Rep.* **2015**, *5*, 1.

[45] J. Zirzlmeier, D. Lehnherr, P. B. Coto, E. T. Chernick, R. Casillas, B. S. Basel, M. Thoss, R. R. Tykwinski, D. M. Guldi, *Proc. Natl. Acad. Sci. U.S.A* **2015**, *112*, 5325.

[46] J. C. Goldschmidt, S. Fischer, *Adv. Opt. Mater.* **2015**, *3*, 510.

[47] L. Frazer, J. K. Gallaher, T. W. Schmidt, *ACS Energy Lett.* **2017**, *2*, 1346.

[48] Q. Wei, N. Fei, A. Islam, T. Lei, L. Hong, R. Peng, X. Fan, L. Chen, P. Gao, Z. Ge, *Adv. Opt. Mater.* **2018**, *6*, 1800512.

[49] P. K. Chow, C. Ma, W. P. To, G. S. M. Tong, S. L. Lai, S. C. Kui, W. M. Kwok, C. M. Che, *Angew. Chem. Int. Ed.* **2013**, *52*, 11775.

[50] Q. Zhang, Q. Zhou, Y. Cheng, L. Wang, D. Ma, X. Jing, F. Wang, *Adv. Mater.* **2004**, *16*, 432.

[51] H. Uoyama, K. Goushi, K. Shizu, H. Nomura, C. Adachi, *Nature* **2012**, *492*, 234.

[52] T.-L. Wu, M.-J. Huang, C.-C. Lin, P.-Y. Huang, T.-Y. Chou, R.-W. Chen-Cheng, H.-W. Lin, R.-S. Liu, C.-H. Cheng, *Nat. Photonics* **2018**, *12*, 235.

[53] H. Liu, Q. Bai, L. Yao, H. Zhang, H. Xu, S. Zhang, W. Li, Y. Gao, J. Li, P. Lu, *Chem. Sci.* **2015**, *6*, 3797.

[54] S. Zhang, L. Yao, Q. Peng, W. Li, Y. Pan, R. Xiao, Y. Gao, C. Gu, Z. Wang, P. Lu, *Adv. Funct. Mater.* **2015**, *25*, 1755.

[55] D. Hu, L. Yao, B. Yang, Y. Ma, *Philos. Trans. R. Soc. A* **2015**, *373*, 20140318.

[56] Y. Pan, W. Li, S. Zhang, L. Yao, C. Gu, H. Xu, B. Yang, Y. Ma, *Adv. Opt. Mater.* **2014**, *2*, 510.

[57] H. Guo, Q. Peng, X.-K. Chen, Q. Gu, S. Dong, E. W. Evans, A. J. Gillett, X. Ai, M. Zhang, D. Credgington, *Nat. Mater.* **2019**, *18*, 977.

[58] L. Song, Y. Hu, Z. Liu, Y. Lv, X. Guo, X. Liu, *ACS Appl. Mater. Interfaces* **2017**, *9*, 2711.

[59] J. Sobus, F. Bencheikh, M. Mamada, R. Wawrzinek, J.-C. Ribierre, C. Adachi, S.-C. Lo, E. B. Namdas, *Adv. Funct. Mater.* **2018**, *28*, 1800340.

[60] X. Ai, E. W. Evans, S. Dong, A. J. Gillett, H. Guo, Y. Chen, T. J. Hele, R. H. Friend, F. Li, *Nature* **2018**, *563*, 536.

[61] Y. Xu, P. Xu, D. Hu, Y. Ma, *Chem. Soc. Rev.* **2020**, *50*, 1030.

[62] Y. Wang, W. Wang, Z. Huang, H. Wang, J. Zhao, J. Yu, D. Ma, *J. Mater. Chem. C* **2018**, *6*, 7042.

[63] H. Chen, X. Xing, J. Miao, C. Zhao, M. Zhu, J. Bai, Y. He, H. Meng, *Adv. Opt. Mater.* **2020**, *8*, 1901651.

[64] V. Ahmad, J. Sobus, F. Bencheikh, M. Mamada, C. Adachi, S. C. Lo, E. B. Namdas, *Adv. Opt. Mater.* **2020**, *8*, 2000554.

[65] Y. Im, S. Y. Byun, J. H. Kim, D. R. Lee, C. S. Oh, K. S. Yook, J. Y. Lee, *Adv. Funct. Mater.* **2017**, *27*, 1603007.

[66] C. Parker, C. Hatchard, *J. Phys. Chem.* **1962**, *66*, 2506.

[67] J. Zhao, S. Ji, H. Guo, *RSC Adv.* **2011**, *1*, 937.

[68] S. H. Lee, M. A. Ayer, R. Vadrucci, C. Weder, Y. C. Simon, *Polym. Chem.* **2014**, *5*, 6898.

[69] A. Monguzzi, R. Tubino, F. Meinardi, *Phys. Rev. B* **2008**, *77*, 155122.

[70] J. Park, M. Xu, F. Li, H. C. Zhou, *J. Am. Chem. Soc.* **2018**, *140*, 5493.

[71] Y. Y. Cheng, A. Nattestad, T. F. Schulze, R. W. MacQueen, B. Fückel, K. Lips, G. G. Wallace, T. Khoury, M. J. Crossley, T. W. Schmidt, *Chem. Sci.* **2016**, *7*, 559.

[72] J. H. Kim, J. H. Kim, *J. Am. Chem. Soc.* **2012**, *134*, 17478.

[73] Q. Liu, T. Yang, W. Feng, F. Li, *J. Am. Chem. Soc.* **2012**, *134*, 5390.

[74] D. Yildiz, C. Baumann, A. Mikosch, A. J. Kuehne, A. Herrmann, R. Göstl, *Angew. Chem. Int. Ed.* **2019**, *58*, 12919.

[75] H. Shang, H. Shimotani, T. Kanagasekaran, K. Tanigaki, *ACS Appl. Mater. Interfaces* **2019**, *11*, 20200.

[76] S. H. C. Askes, B. Sylvestre, *Nat. Rev. Chem.* **2018**, *2*, 437.

[77] B. D. Ravetz, A. B. Pun, E. M. Churchill, D. N. Congreve, T. Rovis, L. M. Campos, *Nature* **2019**, *565*, 343.

[78] T. F. Schulze, J. Czolk, Y. Y. Cheng, B. Fückel, R. W. MacQueen, T. Khoury, M. J. Crossley, B. Stannowski, K. Lips, U. Lemmer, A. Colsmann, T. W. Schmidt, *J. Phys. Chem. C* **2012**, *116*, 22794.

[79] C. E. McCusker, F. N. Castellano, *Top Curr. Chem.* **2016**, *374*, 175.

[80] J. Pedrini, A. Monguzzi, *J. Photonics Energy* **2017**, *8*, 022005.

[81] V. Gray, D. Dzebo, M. Abrahamsson, B. Albinsson, K. Moth-Poulsen, *Phys. Chem. Chem. Phys.* **2014**, *16*, 10345.

[82] Y. Zhang, S. R. Forrest, *Phys. Rev. Lett.* **2012**, *108*, 267404.

[83] D. Di, L. Yang, J. M. Richter, L. Meraldi, R. M. Altamimi, A. Y. Alyamani, D. Credgington, K. P. Musselman, J. L. MacManus-Driscoll, R. H. Friend, *Adv. Mater.* **2017**, *29*, 1605987.

[84] D. Y. Kondakov, *J. Soc. Inf. Disp.* **2009**, *17*, 137.

[85] Z. D. Popovic, H. Aziz, *J. Appl. Phys.* **2005**, *98*, 013510.

[86] Y.-J. Luo, Z.-Y. Lu, Y. Huang, *Chin. Chem. Lett.* **2016**, *27*, 1223.

[87] X. Qiao, D. Ma, *Mater. Sci. Eng. R Rep.* **2020**, *139*, 100519.

[88] M. Zhu, C. Yang, *Chem. Soc. Rev.* **2013**, *42*, 4963.

[89] D. Y. Kondakov, *Philos. Trans. R. Soc. A* **2015**, *373*, 20140321.

[90] S. Engmann, A. J. Barito, E. G. Bittle, N. C. Giebink, L. J. Richter, D. J. Gundlach, *Nat. Commun.* **2019**, *10*, 1.

[91] T. Suzuki, Y. Nonaka, T. Watabe, H. Nakashima, S. Seo, S. Shitagaki, S. Yamazaki, *Jpn. J. Appl. Phys* **2014**, *53*, 052102.

[92] A. Soman, M. M, K. N. N. Unni, *Opt. Mater.* **2018**, *79*, 413.

[93] T. N. Singh-Rachford, F. N. Castellano, *Coord. Chem. Rev.* **2010**, *254*, 2560.

[94] J. Zhao, S. Ji, H. Guo, *RSC Adv.* **2011**, *1*, 937.

[95] J. Zhao, W. Wu, J. Sun, S. Guo, *Chem. Soc. Rev.* **2013**, *42*, 5323.

[96] V. Gray, K. Moth-Poulsen, B. Albinsson, M. Abrahamsson, *Coord. Chem. Rev.* **2018**, *362*, 2560.

[97] L. Huang, E. Kakadiaris, T. Vaneckova, K. Huang, M. Vaculovicova, G. Han, *Biomaterials* **2019**, *201*, 77.

[98] J. Zhou, Q. Liu, W. Feng, Y. Sun, F. Li, *Chem. Rev.* **2015**, *115*, 395.

[99] N. Kimizuka, N. Yanai, M. A. Morikawa, *Langmuir* **2016**, *32*, 12304.

[100] N. Yanai, N. Kimizuka, *Chem. Comm.* **2016**, *52*, 5354.

[101] T. N. Singh-Rachford, A. Haefele, R. Ziessel , F. N. Castellano, *J. Am. Chem. Soc.* **2008**, *130*, 16164.

[102] J. Birks, *Phys. Lett. A* **1967**, *24*, 479.

[103] R. Ieuji, K. Goushi, C. Adachi, *Nat. Commun.* **2019**, *10*, 1.

[104] Y. Y. Cheng, B. Fückel, T. Khoury, R. G. C. R. Clady, M. J. Y. Tayebjee, N. J. Ekins-Daukes, M. J. Crossley, T. W. Schmidt, *J. Phys. Chem. Lett.* **2010**, *1*, 1795.

[105] C. J. Chiang, A. Kimyonok, M. K. Etherington, G. C. Griffiths, V. Jankus, F. Turksoy, A. P. Monkman, *Adv. Funct. Mater.* **2013**, *23*, 739.

[106] F. Deng, J. r. Blumhoff, F. N. Castellano, *J. Mater. Chem. A* **2013**, *117*, 4412.

[107] Y. Y. Cheng, T. Khoury, R. G. Clady, M. J. Tayebjee, N. J. Ekins-Daukes, M. J. Crossley, T. W. Schmidt, *Phys. Chem. Chem. Phys.* **2010**, *12*, 66.

[108] T. W. Schmidt, F. N. Castellano, *J. Phys. Chem. Lett.* **2014**, *5*, 4062.

[109] S. Hoseinkhani, R. Tubino, F. Meinardi, A. Monguzzi, *Phys. Chem. Chem. Phys.* **2015**, *17*, 4020.

[110] A. Haefele, J. Blumhoff, R. S. Khnayzer, F. N. Castellano, *J. Phys. Chem. Lett.* **2012**, *3*, 299.

[111] A. Monguzzi, J. Mezyk, F. Scotognella, R. Tubino, F. Meinardi, *Phys. Rev. B* **2008**, *78*, 195112.

[112] S. M. Bachilo, R. B. Weisman, *J. Phys. Chem. A* **2000**, *104*, 7711.

[113] X. Qiao, P. Yuan, D. Ma, T. Ahamad, S. M. Alshehri, *Org. Electron.* **2017**, *46*, 1.

[114] Y. Zhou, F. N. Castellano, T. W. Schmidt, K. Hanson, *ACS Energy Lett.* **2020**, *5*, 2322.

[115] T. A. Lin, C. F. Perkinson, M. A. Baldo, *Adv. Mater.* **2020**, *32*, 1908175.

[116] M. H. Shubbak, *Renew. Sustain. Energy Rev.* **2019**, *115*, 109383.

[117] T. D. Lee, A. U. Ebong, *Renew. Sustain. Energy Rev.* **2017**, *70*, 1286.

[118] T. F. Schulze, Y. Y. Cheng, B. Fückel, R. W. MacQueen, A. Danos, N. J. L. K. Davis, M. J. Y. Tayebjee, T. Khoury, R. G. C. R. Clady, N. J. Ekins-Daukes, M. J. Crossley, B. Stannowski, K. Lips, T. W. Schmidt, *Aust. J. Chem.* **2012**, *65*, 480.

[119] P. Bi, S. Zhang, J. Wang, J. Ren, J. Hou, *Chin. J. Chem.* **2021**, *39, 10.1002/cjoc.202000666.*

[120] R. R. Islangulov, D. V. Kozlov, F. N. Castellano, *Chem. Comm.* **2005**, 3776.

[121] D. V. Kozlov, F. N. Castellano, *Chem. Comm.* **2004**, 2860.

[122] L. Nienhaus, J.-P. Correa-Baena, S. Wieghold, M. Einzinger, T.-A. Lin, K. E. Shulenberger, N. D. Klein, M. Wu, V. Bulović, T. Buonassisi, *ACS Energy Lett.* **2019**, *4*, 888.

[123] V. Gray, P. Xia, Z. Huang, E. Moses, A. Fast, D. A. Fishman, V. I. Vullev, M. Abrahamsson, K. Moth-Poulsen, M. L. Tang, *Chem. Sci.* **2017**, *8*, 5488.

[124] Z. Huang, Z. Xu, M. Mahboub, Z. Liang, P. Jaimes, P. Xia, K. R. Graham, M. L. Tang, T. Lian, *J. Am. Chem. Soc.* **2019**, *141*, 9769.

[125] J. De Roo, Z. Huang, N. J. Schuster, L. S. Hamachi, D. N. Congreve, Z. Xu, P. Xia, D. A. Fishman, T. Lian, J. S. Owen, *Chem. Mater.* **2020**, *32*, 1461.

[126] T. C. Wu, D. N. Congreve, M. A. Baldo, *Appl. Phys. Lett.* **2015**, *107*, 031103.

[127] D. Wei, F. Ni, Z. Zhu, Y. Zou, C. Yang, *J. Mater. Chem. C* **2017**, *5*, 12674.

[128] A. Ronchi, C. Capitani, V. Pinchetti, G. Gariano, M. L. Zaffalon, F. Meinardi, S. Brovelli, A. Monguzzi, *Adv. Mater.* **2020**, *32*, 2002953.

[129] P. Xia, E. K. Raulerson, D. Coleman, C. S. Gerke, L. Mangolini, M. L. Tang, S. T. Roberts, *Nat. Chem.* **2020**, *12*, 137.

[130] J. Xiang, Y. Chen, W. Jia, L. Chen, Y. Lei, Q. Zhang, Z. Xiong, *Org. Electron.* **2016**, *28*, 94.

[131] H. W. Bae, G. W. Kim, R. Lampande, J. H. Park, I. J. Ko, H. J. Yu, C. Y. Lee, J. H. Kwon, *Org. Electron.* **2019**, *70*, 1.

[132] Dzebo D., Börjesson K., Gray V., Moth-Poulsen K., A. B., *J. Phys. Chem. C* **2016**, *120*, 23397.

[133] P. Keivanidis, S. Baluschev, G. Lieser, G. Wegner, *ChemPhysChem* **2009**, *10*, 2316.

[134] T. Serevičius, R. Komskis, P. Adomenas, O. Adomeniene, V. Jankauskas, A. Gruodis, K. Kazlauskas, S. Jursenas, *Phys. Chem. Chem. Phys.* **2014**, *16*, 7089.

[135] C. Gao, S. K. Prasad, B. Zhang, M. Dvořák, M. J. Tayebjee, D. R. McCamey, T. W. Schmidt, T. A. Smith, W. W. Wong, *J. Phys. Chem. C* **2019**, *123*, 20181.

[136] C. Gao, J. Y. Seow, B. Zhang, C. R. Hall, A. J. Tilley, J. M. White, T. A. Smith, W. W. Wong, *ChemPlusChem* **2019**, *84*, 746.

[137] C. Gao, B. Zhang, C. R. Hall, L. Li, Y. Chen, Y. Zeng, T. A. Smith, W. W. Wong, *Phys. Chem. Chem. Phys.* **2020**, *22*, 6300.

[138] A. B. Pan, S. N. Sanders, M. Y. Sfeir, L. M. Campos, D. N. Congreve, *Chem. Sci.* **2019**, *10*, 3969.

[139] S. Baluschev, T. Miteva, V. Yakutkin, G. Nelles, A. Yasuda, G. Wegner, *Phys. Rev. Lett.* **2006**, *97*, 143903.

[140] A. J. Tilley, B. E. Robotham, R. P. Steer, K. P. Ghiggino, *Chem. Phys. Lett.* **2015**, *618*, 198.

[141] A. J. Tilley, M. J. Kim, M. Chen, K. P. Ghiggino, *Polymer* **2013**, *54*, 2865.

[142] T. N. Singh-Rachford, R. R. Islangulov, F. N. Castellano, *J. Phys. Chem. A* **2008**, *112*, 3906.

[143] T. N. Singh-Rachford, F. N. Castellano, *Inorg. Chem.* **2009**, *48*, 2541.

[144] S. Ji, H. Guo, W. Wu, W. Wu, J. Zhao, *Angew. Chem. Int. Ed.* **2011**, *50*, 8283.

[145] T. N. Singh-Rachford, F. N. Castellano, *J. Phys. Chem. A* **2008**, *112*, 3550.

[146] T. N. Singh-Rachford, F. N. Castellano, *J. Phys. Chem. Lett.* **2010**, *1*, 195.

[147] S. Baluschev, V. Yakutkin, T. Miteva, Y. Avlasevich, S. Chernov, S. Aleshchenkov, G. Nelles, A. Cheprakov, A. Yasuda, K. Müllen, *Angew. Chem. Int. Ed.* **2007**, *46*, 7693.

[148] E. M. Gholizadeh, S. K. K. Prasad, Z. L. Teh, T. Ishwara, S. Norman, A. J. Petty, J. H. Cole, S. Cheong, R. D. Tilley, J. E. Anthony, S. Huang, T. W. Schmidt, *Nat. Photonics* **2020**, *14*, 585.

[149] Y. Y. Cheng, B. Fückel, R. W. MacQueen, T. Khoury, R. G. C. R. Clady, T. F. Schulze, N. J. Ekins-Daukes, M. J. Crossley, B. Stannowski, K. Lips, T. W. Schmidt, *Energy Environ. Sci.* **2012**, *5*, 6953.

[150] A. Nattestad, Y. Y. Cheng, R. W. MacQueen, T. F. Schulze, F. W. Thompson, A. J. Mozer, B. Fückel, T. Khoury, M. J. Crossley, K. Lips, G. G. Wallace, T. W. Schmidt, *J. Phys. Chem. Lett.* **2013**, *4*, 2073.

[151] A. J. Svagan, D. Busko, Y. Avlasevich, G. Glasser, S. Baluschev, K. Landfester, *ACS Nano* **2014**, *8*, 8198.

[152] J.-H. Kim, F. Deng, F. N. Castellano, J.-H. Kim, *ACS Photonics* **2014**, *1*, 382.

[153] O. S. Kwon, J. H. Kim, J. K. Cho, J. H. Kim, *ACS Appl. Mater. Interfaces* **2015**, *7*, 318.

[154] R. Vadrucci, A. Monguzzi, F. Saenz, B. D. Wilts, Y. C. Simon, C. Weder, *Adv. Mater.* **2017**, *29*, 1702992.

[155] C. Wohnhaas, A. Turshatov, V. Mailander, S. Lorenz, S. Baluschev, T. Miteva, K. Landfester, *Macromol. Biosci.* **2011**, *11*, 772.

[156] R. R. Islangulov, J. Lott, C. Weder, F. N. Castellano, *J. Am. Chem. Soc.* **2007**, *129*, 12652.

[157] T. N. Singh-Rachford, J. Lott, C. Weder, F. N. Castellano, *J. Am. Chem. Soc.* **2009**, *131*, 12007.

[158] W. Wu, H. Guo, W. Wu, S. Ji, J. Zhao, *J. Org. Chem.* **2011**, *76*, 7056.

[159] P. B. Merkel, J. P. Dinnocenzo, *J. Phys. Chem. A* **2008**, *112*, 10790.

[160] A. Monguzzi, M. Mauri, A. Bianchi, M. K. Dibbanti, R. Simonutti, F. Meinardi, *J. Phys. Chem. C* **2016**, *120*, 2609.

[161] J. Kim, F. Deng, F. N. Castellano, J. Kim, *Chem. Mater.* **2012**, *24*, 2250.

[162] A. Monguzzi, F. Bianchi, A. Bianchi, M. Mauri, R. Simonutti, R. Ruffo, R. Tubino, F. Meinardi, *Adv. Energy Mater.* **2013**, *3*, 680.

[163] S. H. Lee, J. R. Lott, Y. C. Simon, C. Weder, *J. Mater. Chem. C* **2013**, *1*, 5142.

[164] R. Vadrucci, C. Weder, Y. C. Simon, *J. Mater. Chem. C* **2014**, *2*, 2837.

[165] A. Monguzzi, M. Frigoli, C. Larpent, R. Tubino, F. Meinardi, *Adv. Funct. Mater.* **2012**, *22*, 139.

[166] A. Monguzzi, A. Oertel, D. Braga, A. Riedinger, D. K. Kim, P. N. Knusel, A. Bianchi, M. Mauri, R. Simonutti, D. J. Norris, F. Meinardi, *ACS Appl. Mater. Interfaces* **2017**, *9*, 40180.

[167] S. Raisys, K. Kazlauskas, S. Jursenas, Y. C. Simon, *ACS Appl. Mater. Interfaces* **2016**, *8*, 15732.

[168] P. E. Keivanidis, S. Baluschev, T. Miteva, G. Nelles, U. Scherf, A. Yasuda, G. Wegner, *Adv. Mater.* **2003**, *15*, 2095.

[169] A. Monguzzi, M. Mauri, M. Frigoli, J. Pedrini, R. Simonutti, C. Larpent, G. Vaccaro, M. Sassi, F. Meinardi, *J. Phys. Chem. Lett.* **2016**, *7*, 2779.

[170] R. Vadrucci, C. Weder, Y. C. Simon, *Mater. Horiz.* **2015**, *2*, 120.

[171] S. Baluschev, K. Katta, Y. Avlasevich, K. Landfester, *Mater. Horiz.* **2016**, *3*, 478.

[172] A. Monguzzi, R. Tubino, F. Meinardi, *J. Phys. Chem. A* **2009**, *113*, 1171.

[173] A. L. Hagstrom, F. Deng, J.-H. Kim, *ACS Photonics* **2017**, *4*, 127.

[174] Mengfei Wu, Daniel N. Congreve, Mark W. B. Wilson, Joel Jean, Nadav Geva, Matthew Welborn, Troy Van Voorhis, Vladimir Bulović, Moungi G. Bawendi, M. A. Baldo, *Nat. Photonics* **2015**, *10*, 31.

[175] T. Ogawa, N. Yanai, A. Monguzzi, N. Kimizuka, *Sci. Rep.* **2015**, *5*, 10882.

[176] B. Joarder, N. Yanai, N. Kimizuka, *J. Phys. Chem. Lett.* **2018**, *9*, 4613.

[177] N. Kimizuka, H. Kouno, N. Yanai, T. Ogawa, *J. Photonics Energy* **2017**, *8*, 022003.

[178] P. Duan, N. Yanai, H. Nagatomi, N. Kimizuka, *J. Am. Chem. Soc.* **2015**, *137*, 1887.

[179] P. Duan, N. Yanai, N. Kimizuka, *J. Am. Chem. Soc.* **2013**, *135*, 19056.

[180] T. Ogawa, M. Hosoyamada, B. Yurash, T. Q. Nguyen, N. Yanai, N. Kimizuka, *J. Am. Chem. Soc.* **2018**, *140*, 8788.

[181] S. Hisamitsu, N. Yanai, S. Fujikawa, N. Kimizuka, *Chem. Lett.* **2015**, *44*, 908.

[182] H. Kouno, T. Ogawa, S. Amemori, P. Mahato, N. Yanai, N. Kimizuka, *Chem. Sci.* **2016**, *7*, 5224.

[183] S. Hisamitsu, N. Yanai, N. Kimizuka, *Angew. Chem. Int. Ed.* **2015**, *54*, 11550.

[184] N. Yanai, N. Kimizuka, *Angew. Chem. Int. Ed.* **2020**, *59*, 10252.

[185] S. Amemori, Y. Sasaki, N. Yanai, N. Kimizuka, *J. Am. Chem. Soc.* **2016**, *138*, 8702.

[186] K. Kamada, Y. Sakagami, T. Mizokuro, Y. Fujiwara, K. Kobayashi, K. Narushima, S. Hirata, M. Vacha, *Mater. Horiz.* **2017**, *4*, 83.

[187] L. Li, Y. Zeng, T. Yu, J. Chen, G. Yang, Y. Li, *ChemSusChem* **2017**, *10*, 4610.

[188] C. Li, C. Koenigsmann, F. Deng, A. Hagstrom, C. A. Schmuttenmaer, J.-H. Kim, *ACS Photonics* **2016**, *3*, 784.

[189] Y. L. Lin, M. Koch, A. N. Brigeman, D. M. Freeman, L. Zhao, H. Bronstein, N. C. Giebink, G. D. Scholes, B. P. Rand, *Energy Environ. Sci.* **2017**, *10*, 1465.

[190] J. L. Banal, J. M. White, K. P. Ghiggino, W. W. Wong, *Sci. Rep.* **2014**, *4*, 1.

[191] J. L. Banal, B. Zhang, D. J. Jones, K. P. Ghiggino, W. W. H. Wong, *Acc. Chem. Res.* **2016**, *50*, 49.

[192] J. L. Banal, K. P. Ghiggino, W. W. Wong, *Phys. Chem. Chem. Phys.* **2014**, *16*, 25358.

[193] B. Zhang, C. Gao, H. Soleimaninejad, J. M. White, T. A. Smith, D. J. Jones, K. P. Ghiggino, W. W. Wong, *Chem. Mater.* **2019**, *31*, 3001.

[194] S.-J. Ha, J.-H. Kang, D. H. Choi, S. K. Nam, E. Reichmanis, J. H. Moon, *ACS Photonics* **2018**, *5*, 3621.

[195] K. Kim, S. K. Nam, J. H. Moon, *ACS Appl. Energy Mater.* **2020**, *3*, 5277.

[196] K. Kim, S. K. Nam, J. Cho, J. H. Moon, *Nanoscale* **2020**, *12*, 12426.

[197] S. K. Nam, K. Kim, J. H. Kang, J. H. Moon, *Nanoscale* **2020**, *12*, 17265.

[198] D. Beery, T. W. Schmidt, K. Hanson, *ACS Appl. Mater. Interfaces* **2021**, *13*, 32601.

[199] C. Simpson, T. M. Clarke, R. W. MacQueen, Y. Y. Cheng, A. J. Trevitt, A. J. Mozer, P. Wagner, T. W. Schmidt, A. Nattestad, *Phys. Chem. Chem. Phys.* **2015**, *17*, 24826.

[200] T. Morifuji, Y. Takekuma, M. Nagata, *ACS Omega* **2019**, *4*, 11271.

[201] S. P. Hill, T. Banerjee, T. Dilbeck, K. Hanson, *J. Phys. Chem. Lett.* **2015**, *6*, 4510.

[202] S. P. Hill, T. Dilbeck, E. Baduell, K. Hanson, *ACS Energy Lett.* **2016**, *1*, 3.

[203] S. P. Hill, K. Hanson, *J. Am. Chem. Soc.* **2017**, *139*, 10988.

[204] T. Dilbeck, S. P. Hill, K. Hanson, *J. Mater. Chem. A* **2017**, *5*, 11652.

[205] Y. Zhou, C. Ruchlin, A. J. Robb, K. Hanson, *ACS Energy Lett.* **2019**, *4*, 1458.

[206] K. M. Felter, M. C. Fravventura, E. Koster, R. D. Abellon, T. J. Savenije, F. C. Grozema, *ACS Energy Lett.* **2020**, *5*, 124.

[207] C. Mongin, P. Moroz, M. Zamkov, F. N. Castellano, *Nat. Chem.* **2018**, *10*, 225.

[208] R. Rossetti, J. Ellison, J. Gibson, L. E. Brus, *J. Chem. Phys.* **1984**, *80*, 4464.

[209] Z. Huang, X. Li, B. D. Yip, J. M. Rubalcava, C. J. Bardeen, M. L. Tang, *Chem. Mater.* **2015**, *27*, 7503.

[210] M. Mahboub, Z. Huang, M. L. Tang, *Nano Lett.* **2016**, *16*, 7169.

[211] A. Ronchi, P. Brazzo, M. Sassi, L. Beverina, J. Pedrini, F. Meinardi, A. Monguzzi, *Phys. Chem. Chem. Phys.* **2019**, *21*, 12353.

[212] K. Okumura, K. Mase, N. Yanai, N. Kimizuka, *Chem. Eur. J.* **2016**, *22*, 7721.

[213] D. Beery, J. P. Wheeler, A. Arcidiacono, K. Hanson, *ACS Appl. Energy Mater.* **2019**, *3*, 29.

[214] T. Dilbeck, K. Hanson, *J. Phys. Chem. Lett.* **2018**, *9*, 5810.

[215] T. A. Lin, T. Chatterjee, W. L. Tsai, W. K. Lee, M. J. Wu, M. Jiao, K. C. Pan, C. L. Yi, C. L. Chung, K. T. Wong, C. C. Wu, *Adv. Mater.* **2016**, *28*, 6976.

[216] Y.-L. Shi, M.-P. Zhuo, X.-D. Wang, L.-S. Liao, *ACS Appl. Nano Mater.* **2020**, *3*, 1080.

[217] J. Kido, Y. Iizumi, *Appl. Phys. Lett.* **1998**, *73*, 2721.

[218] V. Jankus, C. J. Chiang, F. Dias, A. P. Monkman, *Adv. Mater.* **2013**, *25*, 1455.

[219] Q. Chen, W. Jia, L. Chen, D. Yuan, Y. Zou, Z. Xiong, *Sci. Rep.* **2016**, *6*, 25331.

[220] C. Xiang, C. Peng, Y. Chen, F. So, *Small* **2015**, *11*, 5439.

[221] B.-Y. Lin, C. J. Easley, C.-H. Chen, P.-C. Tseng, M.-Z. Lee, P.-H. Sher, J.-K. Wang, T.-L. Chiu, C.-F. Lin, C. J. Bardeen, *ACS Appl. Mater. Interfaces* **2017**, *9*, 10963.

[222] N. T. Tierce, C.-H. Chen, T.-L. Chiu, C.-F. Lin, C. J. Bardeen, J.-H. Lee, *Phys. Chem. Chem. Phys.* **2018**, *20*, 27449.

[223] A. Salehi, C. Dong, D.-H. Shin, L. Zhu, C. Papa, A. T. Bui, F. N. Castellano, F. So, *Nat. Commun.* **2019**, *10*, 1.

[224] N. A. Kukhta, T. Matulaitis, D. Volyniuk, K. Ivaniuk, P. Turyk, P. Stakhira, J. V. Grazulevicius, A. P. Monkman, *J. Phys. Chem. Lett.* **2017**, *8*, 6199.

[225] Y. Lei, Y. Zhang, R. Liu, P. Chen, Q. Song, Z. Xiong, *Org. Electron.* **2009**, *10*, 889.

[226] R. Liu, Y. Zhang, Y. Lei, P. Chen, Z. Xiong, *J. Appl. Phys.* **2009**, *105*, 093719.

[227] J. Shi, C. W. Tang, *Appl. Phys. Lett.* **2002**, *80*, 3201.

[228] C. H. Chen, N. T. Tierce, M. k. Leung, T. L. Chiu, C. F. Lin, C. J. Bardeen, J. H. Lee, *Adv. Mater.* **2018**, *30*, 1804850.

[229] J. C. Johnson, A. J. Nozik, J. Michl, *Acc. Chem. Res.* **2013**, *46*, 1290.

[230] S. Karak, J. A. Lim, S. Ferdous, V. V. Duzhko, A. L. Briseno, *Adv. Funct. Mater.* **2014**, *24*, 1039.

[231] P. S. Jo, D. T. Duong, J. Park, R. Sinclair, A. Salleo, *Chem. Mater.* **2015**, *27*, 3979.

[232] G. B. Piland, J. J. Burdett, D. Kurunthu, C. J. Bardeen, *J. Phys. Chem. C* **2013**, *117*, 1224.

[233] P. Chen, Y. Lei, Q. Song, Y. Zhang, R. Liu, Q. Zhang, Z. Xiong, *Appl. Phys. Lett.* **2009**, *95*, 310.

[234] W. Jia, Q. Chen, L. Chen, D. Yuan, J. Xiang, Y. Chen, Z. Xiong, *J. Phys. Chem. C* **2016**, *120*, 8380.

[235] H. Kuma, C. Hosokawa, *Sci. Technol. Adv. Mater.* **2014**, *15*, 034201.

[236] P.-Y. Chou, H.-H. Chou, Y.-H. Chen, T.-H. Su, C.-Y. Liao, H.-W. Lin, W.-C. Lin, H.-Y. Yen, I.-C. Chen, C.-H. Cheng, *Chem. Comm.* **2014**, *50*, 6869.

[237] H. Lim, H. J. Cheon, G. S. Lee, M. Kim, Y.-H. Kim, J.-J. Kim, *ACS Appl. Mater. Interfaces* **2019**, *11*, 48121.

[238] Y. Y. Lyu, J. Kwak, O. Kwon, S. H. Lee, D. Kim, C. Lee, K. Char, *Adv. Mater.* **2008**, *20*, 2720.

[239] H. Fukagawa, T. Shimizu, N. Ohbe, S. Tokito, K. Tokumaru, H. Fujikake, *Org. Electron.* **2012**, *13*, 1197.

[240] Y.-H. Chen, C.-C. Lin, M.-J. Huang, K. Hung, Y.-C. Wu, W.-C. Lin, R.-W. Chen-Cheng, H.-W. Lin, C.-H. Cheng, *Chem. Sci.* **2016**, *7*, 4044.

[241] D. Kabra, L. P. Lu, M. H. Song, H. J. Snaith, R. H. Friend, *Adv. Mater.* **2010**, *22*, 3194.

[242] X. Yang, X. Xu, G. Zhou, *J. Mater. Chem. C* **2015**, *3*, 913.

[243] Z. Xu, B. Z. Tang, Y. Wang, D. Ma, *J. Mater. Chem. C* **2020**, *8*, 2614.

[244] J. K. Park, K. H. Lee, S. Kang, J. Y. Lee, J. S. Park, J. H. Seo, Y. K. Kim, S. S. Yoon, *Org. Electron.* **2010**, *11*, 905.

[245] J. Huang, J.-H. Su, H. Tian, *J. Mater. Chem.* **2012**, *22*, 10977.

[246] J. Y. Hu, Y. J. Pu, F. Satoh, S. Kawata, H. Katagiri, H. Sasabe, J. Kido, *Adv. Funct. Mater.* **2014**, *24*, 2064.

[247] Y.-H. Kim, D.-C. Shin, S. H. Kim, C. H. Ko, H. S. Yu, Y. S. Chae, S.-K. Kwon, *Adv. Mater.* **2001**, *13*, 1690.

[248] G. Mu, S. Zhuang, W. Zhang, Y. Wang, B. Wang, L. Wang, X. Zhu, *Org. Electron.* **2015**, *21*, 9.

[249] J. Zhou, P. Chen, X. Wang, Y. Wang, Y. Wang, F. Li, M. Yang, Y. Huang, J. Yu, Z. Lu, *Chem. Comm.* **2014**, *50*, 7586.

[250] X. Zheng, Q. Peng, J. Lin, Y. Wang, J. Zhou, Y. Jiao, Y. Bai, Y. Huang, F. Li, X. Liu, *J. Mater. Chem. C* **2015**, *3*, 6970.

[251] X. Tang, Q. Bai, T. Shan, J. Li, Y. Gao, F. Liu, H. Liu, Q. Peng, B. Yang, F. Li, *Adv. Funct. Mater.* **2018**, *28*, 1705813.

[252] H. Liu, L. Kang, J. Li, F. Liu, X. He, S. Ren, X. Tang, C. Lv, P. Lu, *J. Mater. Chem. C* **2019**, *7*, 10273.

[253] W. Liu, S. Ying, R. Guo, X. Qiao, P. Leng, Q. Zhang, Y. Wang, D. Ma, L. Wang, *J. Mater. Chem. C* **2019**, *7*, 1014.

[254] R. Kim, S. Lee, K.-H. Kim, Y.-J. Lee, S.-K. Kwon, J.-J. Kim, Y.-H. Kim, *Chem. Comm.* **2013**, *49*, 4664.

[255] M. Jung, J. Lee, H. Jung, S. Kang, A. Wakamiya, J. Park, *Dyes Pigm.* **2018**, *158*, 42.

[256] H. W. Lee, J. Kim, Y. S. Kim, S. E. Lee, Y. K. Kim, S. S. Yoon, *Dyes Pigm.* **2015**, *123*, 363.

[257] M. Muccini, W. Koopman, S. Toffanin, *Laser Photonics Rev.* **2012**, *6*, 258.

[258] R. Capelli, S. Toffanin, G. Generali, H. Usta, A. Facchetti, M. Muccini, *Nat. Mater.* **2010**, *9*, 496.

[259] M. C. Gwinner, D. Kabra, M. Roberts, T. J. K. Brenner, B. H. Wallikewitz, C. R. McNeill, R. H. Friend, H. Sirringhaus, *Adv. Mater.* **2012**, *24*, 2728.

[260] A. Hepp, H. Heil, W. Weise, M. Ahles, R. Schmechel, H. von Seggern, *Phys. Rev. Lett.* **2003**, *91*, 157406.

[261] J. Zaumseil, R. H. Friend, H. Sirringhaus, *Nat. Mater.* **2006**, *5*, 69.

[262] B. B. Y. Hsu, C. Duan, E. B. Namdas, A. Gutacker, J. D. Yuen, F. Huang, Y. Cao, G. C. Bazan, I. D. W. Samuel, A. J. Heeger, *Adv. Mater.* **2012**, *24*, 1171.

[263] L. Hou, X. Zhang, G. F. Cotella, G. Carnicella, M. Herder, B. M. Schmidt, M. Paetzel, S. Hecht, F. Cacialli, P. Samori, *Nat. Nanotechnol.* **2019**, *14*, 347.

[264] R. Ding, M. H. An, J. Feng, H. B. Sun, *Laser Photonics Rev.* **2019**, *13*, 1900009.

[265] C. Zhang, P. Chen, W. Hu, *Small* **2016**, *12*, 1252.

[266] J. Liu, Z. Qin, H. Gao, H. Dong, J. Zhu, W. Hu, *Adv. Funct. Mater.* **2019**, *29*, 1808453.

[267] Z. Qin, H. Gao, H. Dong, W. Hu, *Adv. Mater.* **2021**, *33*, 2007149.

[268] A. Dadvand, A. G. Moiseev, K. Sawabe, W.-H. Sun, B. Djukic, I. Chung, T. Takenobu, F. Rosei, D. F. Perepichka, *Angew. Chem. Int. Ed.* **2012**, *51*, 3837.

[269] J. Liu, H. Zhang, H. Dong, L. Meng, L. Jiang, L. Jiang, Y. Wang, J. Yu, Y. Sun, W. Hu, *Nat. Commun.* **2015**, *6*, 10032.

[270] J. Li, K. Zhou, J. Liu, Y. Zhen, L. Liu, J. Zhang, H. Dong, X. Zhang, L. Jiang, W. Hu, *J. Am. Chem. Soc.* **2017**, *139*, 17261.

[271] Z. Qin, H. Gao, J. Liu, K. Zhou, J. Li, Y. Dang, L. Huang, H. Deng, X. Zhang, H. Dong, W. Hu, *Adv. Mater.* **2019**, *31*, 1903175.

[272] D. Liu, J. De, H. Gao, S. Ma, Q. Ou, S. Li, Z. Qin, H. Dong, Q. Liao, B. Xu, Qian Peng, Zhigang Shuai, Wenjing Tian, Hongbing Fu, Xiaotao Zhang, Yonggang Zhen, W. Hu, *J. Am. Chem. Soc.* **2020**, *142*, 6332.

[273] H. Ju, K. Wang, J. Zhang, H. Geng, Z. Liu, G. Zhang, Y. Zhao, D. Zhang, *Chem. Mater.* **2017**, *29*, 3580.

[274] M. Chen, Y. Zhao, L. Yan, S. Yang, Y. Zhu, I. Murtaza, G. He, H. Meng, W. Huang, *Angew. Chem. Int. Ed.* **2017**, *56*, 722.

[275] J. Liu, J. Liu, Z. Zhang, C. Xu, Q. Li, K. Zhou, H. Dong, X. Zhang, W. Hu, *J. Mater. Chem. C* **2017**, *5*, 2519.

[276] J. Li, J. Liu, Y. Zhen, L. Meng, Y. Wang, H. Dong, W. Hu, *J. Mater. Chem. C* **2015**, *3*, 10695.

[277] L. Zheng, J. Li, K. Zhou, X. Yu, X. Zhang, H. Dong, W. Hu, *Nano Res.* **2020**, *13*, 1976.

[278] Z. Xie, D. Liu, Y. Zhang, Q. Liu, H. Dong, W. Hu, *Chem. Res. Chin. Univ* **2020**, *41*, 1179.

[279] E. B. Namdas, B. B. Y. Hsu, Z. Liu, S.-C. Lo, P. L. Burn, I. D. W. Samuel, *Adv. Mater.* **2009**, *21*, 4957.

[280] M. Ullah, K. Tandy, A. J. Clulow, P. L. Burn, I. R. Gentle, P. Meredith, S.-C. Lo, E. B. Namdas, *ACS Photonics* **2017**, *4*, 754.

[281] R. Wawrzinek, K. Muhieddine, M. Ullah, P. B. Koszo, P. E. Shaw, A. Grosjean, F. Maasoumi, D. M. Stoltzfus, J. K. Clegg, P. L. Burn, E. B. Namdas, S.-C. Lo, *Adv. Opt. Mater.* **2016**, *4*, 1867.

[282] M. Ullah, S. D. Yambem, E. G. Moore, E. B. Namdas, A. K. Pandey, *Adv. Electron. Mater.* **2015**, *1*, 1500229.

[283] T. Takenobu, S. Z. Bisri, T. Takahashi, M. Yahiro, C. Adachi, Y. Iwasa, *Phys. Rev. Lett.* **2008**, *100*.

[284] P. M. Zimmerman, Z. Zhang, C. B. Musgrave, *Nat. Chem.* **2010**, *2*, 648.

[285] P. M. Zimmerman, F. Bell, D. Casanova, M. Head-Gordon, *J. Am. Chem. Soc.* **2011**, *133*, 19944.

[286] J. J. Burdett, A. M. Müller, D. Gosztola, C. J. Bardeen, *J. Chem. Phys.* **2010**, *133*, 144506.

[287] F. Qiu, Y. Dong, J. Liu, Y. Sun, H. Geng, H. Zhang, D. Zhu, X. Shi, J. Liu, J. Zhang, S. Ai, L. Jiang, *J. Mater. Chem. C* **2020**, *8*, 6006.

[288] Z. Liu, G. Zhang, D. Zhang, *Chem. Eur. J.* **2016**, *22*, 462.

[289] D. Yuan, V. Sharapov, X. Liu, L. Yu, *ACS Omega* **2019**, *5*, 68.

[290] Z. H. Wu, Z. T. Huang, R. X. Guo, C. L. Sun, L. C. Chen, B. Sun, Z. F. Shi, X. Shao, H. Li, H. L. Zhang, *Angew. Chem. Int. Ed.* **2017**, *56*, 13031.

[291] R. Ding, X. P. Wang, J. Feng, X. B. Li, F. X. Dong, W. Q. Tian, J. R. Du, H. H. Fang, H. Y. Wang, T. Yamao, S. Hotta, H. B. Sun, *Adv. Mater.* **2018**, *30*, 1801078.

[292] H. Nakanotani, M. Saito, H. Nakamura, C. Adachi, *Adv. Funct. Mater.* **2010**, *20*, 1610.

[293] I. Salzmann, G. Heimel, M. Oehzelt, S. Winkler, N. Koch, *Acc. Chem. Res.* **2016**, *49*, 370.

[294] B. Lussem, C. M. Keum, D. Kasemann, B. Naab, Z. Bao, K. Leo, *Chem. Rev.* **2016**, *116*, 13714.

[295] I. E. Jacobs, A. J. Moule, *Adv. Mater.* **2017**, *29*, 1703063.

[296] H. Nakanotani, T. Furukawa, T. Hosokai, T. Hatakeyama, C. Adachi, *Adv. Opt. Mater.* **2017**, *5*, 1700051.

[297] Z. Yu, Y. Wu, L. Xiao, J. Chen, Q. Liao, J. Yao, H. Fu, *J. Am. Chem. Soc.* **2017**, *139*, 6376.

[298] H. Nakanotani, T. Furukawa, C. Adachi, *Adv. Opt. Mater.* **2015**, *3*, 1381.

[299] J. Xue, Q. Liang, R. Wang, J. Hou, W. Li, Q. Peng, Z. Shuai, J. Qiao, *Adv. Mater.* **2019**, *31*, 1808242.

[300] X. K. Chen, Y. Tsuchiya, Y. Ishikawa, C. Zhong, C. Adachi, J. L. Bredas, *Adv. Mater.* **2017**, *29*, 1702767.

[301] A. Shukla, M. Hasan, G. Banappanavar, V. Ahmad, J. Sobus, E. G. Moore, D. Kabra, S.-C. Lo, E. B. Namdas, **2021**, *DOI: 10.21203/rs.3.rs-74957/v1*.

[302] J. Liu, H. Dong, Z. Wang, D. Ji, C. Cheng, H. Geng, H. Zhang, Y. Zhen, L. Jiang, H. Fu, Z. Bo, W. Chen, Z. Shuai, W. Hu, *Chem. Commun.* **2015**, *51*, 11777.

[303] A. B. Pun, L. M. Campos, D. N. Congreve, *J. Am. Chem. Soc.* **2019**, *141*, 3777.

Can Gao is currently a postdoctoral researcher in the Institute of Chemistry, Chinese Academy of Sciences. She completed her Master's degree in the University of Chinese Academy of Sciences in 2015, and Ph.D. in the

University of Melbourne, Australia in 2019. Her research interests are focused on the development of organic light-emitting transistor materials and investigation of their photoelectric properties.

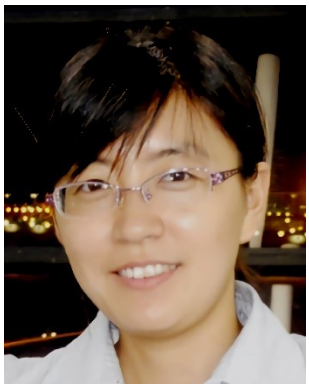

Huanli Dong is a Professor of Institute of Chemistry, Chinese Academy of Sciences. She received her Ph.D. degree from the Institute in 2009 after she got her M.S. degree from Fujian Institute of Research on the Structure of Material, CAS, in 2006. Her current research focuses on organic semiconductor crystals including organic small molecules and conjugated polymers by material science and growth technology and their applications in OFETs, integrated optoelectronic devices, and circuits.

WILEY-VCH

TOC

A comprehensive summary of intriguing advances on developing efficient triplet-triplet annihilation (TTA) upconversion materials and their application in optoelectronic devices is systematically given along with discussions in this review. The key challenges and perspectives of TTA upconversion systems for further improvement for optoelectronic devices and other related research directions are provided. This review hopes to provide valuable guidelines for future related research and advancement in organic optoelectronics.